Monitoring the Crosstalk between Methylation and Phosphorylation on Histone Peptides with Host-Assisted Capillary Electrophoresis

Jiwon Lee<sup>1</sup>, Junyi Chen<sup>2</sup>, Priyanka Sarkar<sup>1</sup>, Min Xue<sup>1,2</sup>, Richard J. Hooley<sup>1,3</sup>, Wenwan Zhong<sup>1,2</sup>

<sup>1</sup>Department of Chemistry, University of California-Riverside, 900 University Ave., Riverside, California, 92521, USA

<sup>2</sup>Department of Environmental Toxicology Program, University of California-Riverside, 900 University Ave., Riverside, CA 92521, USA

<sup>3</sup>Department of Biochemistry and Molecular Biology, University of California-Riverside, 900 University Ave., Riverside, CA 92521, USA

\*Correspondence: wenwan.zhong@ucr.edu

Keywords: Capillary electrophoresis · enzyme assay · post-translational modification · PTM crosstalk · synthetic receptor

#### Abstract

Post-translational modifications (PTMs) greatly increase protein diversity and regulate their functions by changing the structures, properties, and molecular interactions of proteins. In peptide regions with high density of PTMs, PTMs can influence modification on residues in proximity or even at distal positions, adding another layer of regulation. Methods that can monitor the activities of PTM enzymes on peptides carrying multiple modifications are valuable tools for better understanding of PTM crosstalk. Herein, we developed a host-assisted capillary electrophoresis (CE) method to separate histone peptides with methylation and phosphorylation and applied it to monitor the crosstalk between serine phosphorylation and lysine methylation when they are added by Aurora B kinase and G9a lysine methyltransferase, respectively. A synthetic receptor molecule, 4-hexasulfonatocalix[6] arene (CX6), was included in the CE buffer to improve the resolution of the corresponding substrates and products. A linear polyacrylamidecoated capillary was employed to effectively reduce wall adsorption of the cationic histone peptides. The peptide substrates were labeled with fluorescein to enhance their detectability during CE separation. Our method successfully revealed that the activity of G9a methyltransferase was completely inhibited by the adjacent phosphorylation, while 25% reduction in the activity of Aurora B kinase was observed with the presence of the demethylation on the nearby residue. The PTM crosstalk was examined not only using a pure peptide substrate, but also in a competitive reaction environment, in which the modified and unmodified peptides were mixed and the enzyme actions on both peptides were monitored simultaneously. Our work demonstrates that host-assisted CE is an effective method for study of PTM crosstalk, which could offer the advantages of fast separation, high resolution, and low sample consumption.

# Introduction

Post-translational modification (PTM) on proteins greatly increase their diversity by changing the structures, properties, and interactions, leading to substantial effects on activity. There are various PTM classifications including phosphorylation, methylation, glycosylation, and ubiquitination [1]. While PTMs can occur on all proteins, the ones on histone proteins that condense DNA into chromatin can affect gene expression. These PTMs are important epigenetic factors to regulate cellular functions like development, differentiation, proliferation, and apoptosis. They also respond to different stimuli, leading to altered biological processes and development of pathological conditions. Therefore, monitoring PTM changes in histone proteins is essential for better understanding of the regulation mechanisms of cellular processes.

PTMs are controlled by modification enzymes, which can act as "writers" to add the specific PTM or as "erasers" to remove it. Furthermore, the activity of PTM enzymes can be affected by pre-existing modifications, termed crosstalk. In crosstalk events occurring to histone proteins, one PTM can directly interfere with or enhance the addition of another mark located within the same [2] or another histone protein [3, 4], leading to downstream effects in chromatin structure and gene expression, as well as eventually inducing pathological development. To elucidate the crosstalk events among PTMs, we can compare the activity of enzymes on substrates with or without other modifications.

Current methods for monitoring enzymatic activity include spectrophotometric [5, 6] and radiometric [7–9] techniques, however, there can be overlap in the signals of the product and other molecules or safety concerns about radioactive waste. It is also difficult to use these techniques to inspect competition between peptide substrates with or without other modifications in a mixture as well as detect modifications on one of them. Separation techniques that can

resolve peptides with different PTMs are appropriate for studying PTM crosstalk. In particular, capillary electrophoresis (CE) has been widely applied in the study of enzyme activity [10] because of its low sample consumption, capability to monitor reaction in real-time, and potential for high throughput operation. More importantly, its high resolving power is essential in separation of peptides carrying PTMs that confer only small changes in hydrophobicity, size, and charge. CE has been used for separation of peptides in a simpler setting (i.e., single modification, such as phosphorylation or methylation) [11–13]; however, it is still challenging to separate substrates from products with multiple modifications. Therefore, a separation additive is necessary for improved resolution.

Synthetic receptors are recognition units that can form an association complex with their desired targets, such as biomolecules [14]. They can be included in the background electrolytes of CE to improve separation of their target molecules, because of their quick on-and-off binding rate, low molecular weight compared to protein receptors, and good water solubility. With understanding of their interaction with guests, their structures can be designed to improve binding strength and selectivity; furthermore, they can be synthesized with low cost on a large scale. These features are beneficial for obtaining high separation efficiency with simple and low-expense operation. Several supramolecular host molecules, including calixarenes [13, 15-16], cucurbiturils [17], and cavitands [18-20], have shown selectivity for PTMs like methylation and phosphorylation, which supports that synthetic hosts can be exploited to improve CE-based PTM analysis.

While phosphorylation changes the charge of the peptide, it is more challenging for CE to resolve peptides carrying methylation, which adds one to three methyl groups without charge alteration. In our previous work, we successfully developed the host-assisted CE method that

employed 4-tetrasulfonatocalix[4]arene (CX4), 4-hexasulfonatocalix[6]arene (CX6), or cucurbit[7]uril (CB7) in the running buffer of CE to separate peptides with various degrees of lysine methylation. We also briefly demonstrated that this method can be applied to study the activity of methylation enzymes when using histone demethylases as the examples. In this study, the host-assisted CE method can be applied to analyze enzyme crosstalk in a one-pot reaction by simultaneously monitoring the changes on the peptides with or without a pre-existing modification. Using a capillary that was coated with linear polyacrylamide (LPA) and the fluorescently labeled peptides synthesized in-house, we proved that the host-assisted CE method could resolve the peptides carrying multiple modifications. The activities of G9a methyltransferase or Aurora B kinase, which have been reported to be involved in crosstalk events [21-24], were examined in the presence of an antagonistic modification on the adjacent residue. This reveals the effect of phosphorylation on methyltransferase activity and vice versa.

#### Materials and methods

#### Capillary electrophoresis

Separation of non-fluorescently labeled peptides was conducted on an Agilent 7100 CE system with a UV-visible diode-array detector. Data were acquired via ChemStation (Agilent Technologies, Santa Clara, CA). Samples were introduced into the LPA-coated capillary (with an inner and outer diameter of 50 and 365  $\mu$ m, respectively; and an effective length of 26.5 cm) with a 50 mbar injection for 5 s. Separation was driven by an electric field of 571 V/cm with positive polarity and added pressure of 5 mbar. Separation of fluorescently labeled peptides was performed using a Beckman Coulter ProteomeLab PA 800 (Beckman Coulter, Fullerton, CA) with a laser-induced fluorescence (LIF) detector ( $\lambda_{exc}$  = 488 nm,  $\lambda_{em}$  = 520 nm). Samples were

introduced into the LPA-coated capillary (with an inner and outer diameter of 50 and 365  $\mu$ m, respectively; and an effective length of 20 cm) at 0.5 psi for 5 s. Separation was driven by an electric field of 662 V/cm with a positive polarity. Data were acquired via 32 Karat and analyzed via OriginPro 8.6.

#### **Preparation of the Linear Polyacrylamide Coating**

Bare fused-silica capillaries (50 μm i.d., 365 μm o.d.) were purchased from Polymicro Technologies (Phoenix, Arizona). The inner wall of the bare fused silica capillary was coated with linear polyacrylamide, based on a protocol from Zhu *et al.* [25] with several modifications and described as following. The mixture of acrylamide and ammonium persulfate was degassed under the vacuum and flushed through the capillary with nitrogen. The sealed capillary was then incubated in an oven at 50 °C for 30 minutes. After rinsing excess reagents with water, the capillary was dried with nitrogen and stored at room temperature.

#### Enzyme activity and inhibition assays

The lysine methyltransferase assay was carried out using the synthesized, fluorescently labeled peptides: H3 (1-11) peptide with sequence FAM-ARTKQTARKST and H3S10p with sequence FAM-ARTKQTARK-pS-T. Ten μM of FAM-labeled H3 (1-11), FAM-labeled H3S10p, or a mixture of the two was incubated with 0.25 μM human recombinant G9a protein (Sigma-Aldrich, St. Louis, MO) in the reaction buffer, which is composed of 500 μM *s*-(5′-adenosyl)-*L*-methionine (SAM) and 0.1 Mg<sup>2+</sup> in 20 mM tris pH 9.0 at room temperature. The reaction mixture was injected into the LPA-coated capillary at time intervals between 0 and 3

hours and separated with a positive field strength of 662 V/cm in the Beckman PA800 system coupled to an LIF detector.

The kinase assay was carried out using synthesized and fluorescently labeled peptides: FAM-labeled H3 (1-11) peptide with sequence FAM-ARTKQTARKST and FAM-labeled H3K9me<sub>2</sub> with sequence FAM-ARTKQTAR-K(me<sub>2</sub>)-ST. Ten μM of FAM-labeled H3 (1-11), FAM-labeled H3K9me<sub>2</sub>, or a mixture of the two was incubated with 0.01 μg/μL Aurora B kinase (Sigma-Aldrich, St. Louis, MO) in the reaction buffer (20 μM adenosine triphosphate or ATP, 0.1 Mg<sup>2+</sup> in 20 mM tris pH 7.4) at room temperature. For the peptide mixture, 0.005 μg/μL Aurora B was used instead. The reaction mixture was injected into the LPA-coated capillary at time intervals between 0 and 4 hours. A parallel inhibitor experiment was performed with 2.5 nM AZD1152-hydroxyquinazoline pyrazol anilide (Sigma-Aldrich, St. Louis, MO), 10 μM FAM-labeled H3 (1-11), 0.005 μg/μL Aurora B kinase in the reaction buffer (20 μM ATP, 0.1 Mg<sup>2+</sup> in 20 mM tris pH 7.4) at room temperature.

All enzyme assays in this work were monitored in the Beckman PA800 system coupled to an LIF detector, with the CE separation buffer containing 2  $\mu$ M CX6 in 10 mM phosphate at pH 7.4, and a positive field strength of 662 V/cm.

#### Results and discussion

#### Enzymes of interest and their peptide substrates

The present work focused on G9a and Aurora B kinase, which exhibit PTM crosstalk activities. G9a is a histone methyltransferase that has a role in embryonic stem cell differentiation [26], but it is also correlated with metastatic cancer when overexpressed [27]. This enzyme can dimethylate lysine 9. In order for methylation to proceed on lysine 9, G9a

requires at least the following amino acid sequence: TARKSTG [24]. It has been revealed that phosphorylated serine 10 can reduce the activity of G9a to methylate lysine 9 [21, 24], through which H3 phosphorylation could affect gene expression [27] in addition to its commonly known functions in chromatin compaction. On the other hand, a nearby methylated lysine residue can impact phosphorylation on serine, which can occur during catalysis by Aurora B kinase. This protein is involved in the regulation of mitosis events [28] during which it can phosphorylate serine 10. Dimethylation on lysine 9 can have an antagonistic effect on the activity of Aurora B [20, 21]. Aurora B has an important role in the regulation of kinetochore to microtubule attachment [29], so inhibition of the enzyme can interfere with this process.

Both G9a and Aurora B can act on histone proteins but on more than one residue; therefore, we employed histone peptides as the enzyme substrates. We chose to synthesize the peptides for the flexibility in placing multiple modifications at different amino acid sites; however, the yield is limited by the peptide length. A minimum of seven amino acids is required for the G9a substrate [24] while a minimum of 10 amino acids is required for the Aurora B kinase substrate [30]; thus, we synthesized peptides with 11 amino acids that included the target residues to fulfill the substrate requirement of both enzymes (Table S1). Furthermore, we fluorescently labeled the peptides to improve their detectability during CE separation. However, the labeling molecule, carboxyfluorescein (FAM), is comprised of a mixture of both isomers, 5-FAM and 6-FAM, in order to reduce the cost. These cannot be differentiated in the MALDI spectrum due to them bearing the same molecular weight (see Electronic Supplementary Material, or ESM, Fig. S1), but CE can resolve the two isomers. Nevertheless, four peptide substrates for the two selected enzymes could be utilized for studying enzyme crosstalk.

#### Capillary coating to prevent peptide adsorption

Many histone peptides have isoelectric points in the range of 10 to 12. In neutral buffers, they carry positive charges and can be easily adsorbed to the negatively charged silanol groups via electrostatic attraction, which makes it necessary to coat the capillary wall to prevent peak distortion and sample loss. A capillary coating can minimize fluctuation in electroosmotic flow (EOF), which could be induced by adsorption of the added host molecules. Covering the capillary wall can produce more reproducible migration for accurate analyte identification and quantification, which are required for enzyme assays. Coatings can either be dynamic or permanent. Dynamic coating requires inclusion of the coating material in the running buffer, which also contains the synthetic hosts in our host-assisted CE method. This would make the buffer system complicated and reduce repeatability of separation. Therefore, we chose the permanent coating approach in our work.

In our previous work, we used the commercially available, pre-cut capillary coated by polyvinyl alcohol (PVA), which reduced peptide adsorption to the capillary wall and yielded satisfactory resolution of the histone peptides with varied methylation. In the present work, we carried out an in-lab coating of the capillaries using linear polyacrylamide (LPA) to gain more flexibility in usage and better control over the coating quality and reproducibility. Like the PVA coating, the LPA coating is neutral and hydrophilic. It prevents adsorption of both cationic peptides and hydrophobic synthetic hosts. Various buffers, including solvents with surfactants [31] as well as those in a wide pH range from 2-10, can be used in LPA-coated capillaries. These features make the LPA-coated capillaries compatible with diverse synthetic hosts—specifically, the calixarene- and cucurbituril-based hosts used in our work.

We adopted the protocol reported by Dovichi's group to produce the LPA-coated capillaries [25]. In this protocol, 3-(trimethoxysilyl)propyl methacrylate, a bifunctional linker solution was injected into the capillary in order to activate the silanol groups for crosslinking with the polymer. Subsequently, the solution of acrylamide monomer and ammonium persulfate initiator was introduced. Catalysts, such as tetramethylethylenediamine, can be used to promote polymerization. We used heat to catalyze the reaction, because the procedure is simpler and produces more consistent polymerization throughout the length of the capillary. To test the coating's effectiveness, we injected a set of standard proteins with various pI values: cytochrome c (pI = 9.6), lysozyme (pI = 10.7),  $\alpha$ -lactalbumin (pI = 4.8), and hemoglobin (pI = 7.4) (see ESM Fig. S2). Each protein was well separated from the others, and the relative standard deviations for run-to-run migration times and peak areas were less than 6% with triplicate measurements (see ESM Table S2). More importantly, the basic proteins, lysozyme and cytochrome c, did not show significant peak tailing, although they had relatively larger tailing factors (see ESM Equation S1) than the acidic lactalbumin or the neutral hemoglobin.

Successful monitoring of PTM crosstalk relies on the separation of peptides with different methylation levels by incorporating synthetic receptor molecules (see ESM Fig. S3) in the background electrolyte. In order to demonstrate the separation capability of these synthetic receptors in an LPA-coated capillary, we tested the separation of the unlabeled H3K9me<sub>0-3</sub> peptides with CX4 in phosphate buffer at pH 3.0, a condition used in our previous work. The tailing factors and values for resolution (see ESM Equation S2) in the LPA-coated capillary were similar to that of the commercial capillary (see ESM Fig. S4). The relative standard deviation (RSD) for each peptide's migration time was about 0.1-0.2%, and the RSD of the peak area for most peptides was less than 10% except for the unlabeled H3K9me<sub>3</sub> (see ESM Table S3). We

suspect that the synthetic receptor in the background electrolyte, which also adsorbs light in the UV region, contributes to the relatively large variation in peak area. Using fluorescence as the detection method could reduce influence from the background electrolyte and may help improve the reproducibility in quantification. Therefore, in the following study, we prepared and employed the fluorescently labeled peptides in optimization of the host-assisted CE-LIF method and in all enzyme assays.

#### **Optimization of separation**

Our previous work only focused on separation of histone peptides with different methylation levels. The enzyme crosstalk study requires baseline separation of peptides with multiple modifications, so the separation conditions need to be optimized. In addition, the previous method used an acidic buffer at pH 3.0, the working pH recommended for the PVA-coated capillary by the manufacturer; but analysis of a wider scope of PTMs could require a broader pH range for the separation buffer. Moreover, a higher pH would speed up the separation by increasing the EOF, which is significantly suppressed by the coating, induce less positive charges on the histone peptides to prevent wall adsorption, and enhance the quantum yield of the FAM label on the peptides for better detectability in enzyme assays (see ESM Figure S4). Thus, in the present work, we carried out the separation at pH 7.4 and optimized our method to accommodate peptides carrying different combinations of methylation and phosphorylation (see ESM Fig. S5). Under such a pH condition, the LPA coating remains stable: the coated capillary underwent at least 180 runs at pH 7.4 before obvious deterioration in separation performance was observed.

As demonstrated in our previous work, CX4, CX6, and CB7 are effective in separating methylated and unmethylated small guests and peptides. All three synthetic hosts have electron-rich rims and hydrophobic cavities with CX4 and CX6 being negatively charged and CB7 being neutral (see ESM Fig. S3). These synthetic receptors interact with the methyl groups via their hydrophobic cavities [32]. Differences in their molecular structures determine the affinity of these receptors to the methylated peptides, and the separation performance could vary as a result. While CB7 binds more strongly to the trimethylated peptides than CX4 and CX6, the calixarenes can separate all methylation levels better. Out of the previously tested synthetic host molecules, CX6 resulted in the best resolution between all the peptides with different methylation levels [33]. This is most likely due to the added benefit of its higher structural flexibility, more negative charges compared to CX4, and better compatibility between its cavity and the trimethylated lysine.

To confirm the optimal receptor type, we tested the separation performance of each synthetic host, which was added to the background electrolyte at the same molar concentration. With 0.5 μM CX4 or CB7 in the running buffer, the FAM-labeled-H3K9me<sub>0</sub> and H3K9me<sub>2</sub> were not separated; however, inclusion of 0.5 μM CX6 led to separation of the two peptides. Due to binding between CX6 and the methylated peptides, FAM-labeled H3K9me<sub>2</sub> migrated more slowly compared to the unmethylated counterpart (Figure 1a). Although phosphorylation adds negative charges to the peptide, the migration times of the FAM labeled-H3K9me<sub>0</sub>S10p and H3K9me<sub>2</sub>S10p were quite comparable without the host. Only with the addition of CX6, the phosphorylated peptide migrated later than the unmodified one (Fig. 1b), and higher CX6 concentration yielded better resolution (see ESM Fig. S6). On the contrary, a high concentration up to 10 μM of CX4 or CB7 did not lead to any separation.

After determining the best receptor, we tested the effect of buffer composition on the separation capability of CX6 (Fig. 1c and 1d). Tris and phosphate buffers were chosen since pH 7.4 is within their buffering ranges. FAM-labeled H3K9me<sub>0</sub> and H3K9me<sub>2</sub> were separated by CX6 in tris buffer; however, the peptide migration shifts were less than those in the phosphate buffer. CX6 may behave differently in Tris buffer, which contains an amine group akin to the side chain in lysine. For both the FAM-labeled H3K9me<sub>0,2</sub> and H3K9me<sub>0,2</sub>S10p pairs, the resolution was higher in phosphate buffer than in Tris buffer (see ESM Table S4).

#### Lysine methylation on unmodified and phosphorylated peptides

Although 0.5 μM CX6 was adequate to resolve the dimethylated and unmethylated peptide (see ESM Fig. S7), a higher concentration of CX6 at 2 μM was employed in our assay to ensure good separation of the phosphorylated pair as well (see ESM Fig. S6). To confirm that the enzyme and the cofactors did not interfere with the separation, we injected several controls, including a deactivated G9a reaction with spiked dimethylated product (see ESM Figs. S8 and S9). Minimal influence from the cofactors and the deactivated enzyme to the migration and separation of the methylated and unmethylated peptides was observed. When the real enzyme reaction mixture was analyzed, both the mono- and di-methylated peptide peak showed up at the reaction time of 30 min, and the dimethylated peptide became the dominant product at 90 min (Figure 2a). Plotting the percent peak area (dividing the peak area of FAM-labeled H3K9me<sub>x</sub> by the total peak area) against the reaction time showed that the relative content of H3K9me<sub>1</sub> reached the maximum at 30 min and then decreased to zero at 120 min; in contrast, the relative content of H3K9me<sub>2</sub> continued to increase until reaching a plateau (Figure 2c and see ESM Fig. S10c). A pair of peaks started to appear at the 90-minute mark and its intensity remained to be

very low, with its percent peak area reaching only about 10% at 180 minutes. MALDI analysis confirmed that this peak had a m/z of 1648 (see ESM Fig. S10a), which is the mass of the trimethylated peptide. G9a predominantly mono- and di-methylates lysine 9, [34] however, it can trimethylate the residue at a slower rate after the substrate and intermediate are exhausted [35, 36] or when the reaction is left overnight [37]. The high resolution of the methylated peptides provided by the host-assisted CE method enables clear monitoring of the generation and disappearance of the reaction intermediates as well as the side products.

When the substrate was FAM-labeled H3K9me<sub>0</sub>S10p, there was remarkably no product peak even after three hours (Figs. 2b&d and see ESM Figs. S10b&d); this proves that phosphorylated serine 10, when adjacent to lysine 9, blocked the activity of G9a. This result agrees with the literature reports [22-24]. Possible explanations for the inhibitory effect of the phosphate group could be its steric hindrance or repulsion that affects the conformation of the residues, making addition of the methyl group impossible. Since our CE method can separate the phosphorylated peptides with or without methylation, it becomes simple to reveal the crosstalk activity.

Both CE and MALDI could be used to monitor enzyme reactions. The reaction curves obtained from these two methods on the same reaction samples (see ESM Figure S10c) looked similar, but CE seemed to provide better reproducibility, as shown by the smaller error bars in Fig. 2c. While MALDI can have a quick turnaround time and high-throughput capabilities, inconsistent crystal formation between the analyte and the ionization substrate on the MALDI plate could lead to large variations in the resultant signal intensity [38], which could be the main reason for the relatively poor reproducibility observed in our study. Although CE requires fluorescent labeling of samples to produce low detection limits, it has several advantages,

including the capability of *in situ* monitoring (i.e., no quenching treatment of the reaction), low sample consumption, and reliable quantitation.

#### Phosphorylation on unmodified and methylated peptides and enzyme inhibition assay

Likewise, how phosphorylation is affected by nearby methylation can be monitored by our CE method. With 2 μM CX6 in the background electrolyte, good resolution between the FAM-labeled phosphorylated and non-phosphorylated peptides could be achieved, regardless of whether the adjacent lysine carried methylation or not, with the peptides in either a simple buffer or spiked in the complex phosphorylation reaction solution (see ESM Figs. S11-13). Monitoring phosphorylation of the H3 peptides revealed that both H3 and H3K9me<sub>2</sub> were phosphorylated (see ESM Figs. S14 and S15). However, about 25% more phosphorylation was obtained on the unmethylated peptide than on the dimethylated counterpart after 4 hours of reaction time (Fig. 3a), revealing the antagonistic effect on the activity of Aurora B by dimethylation on lysine 9 [20,21]. However, the MALDI results did not reveal such a trend. Large variation from sample crystallization and ionization during MALDI analysis may have prevented monitoring of the enzyme reaction with good quantification accuracy.

The capability of our method to reveal the antagonistic effect of the nearby PTM indicates that it can be used to screen for enzyme inhibitors. As a simple demonstration, we employed AZD1152-hydroxyquinazoline pyrazol anilide (AZD1152-HQPA), a selective inhibitor targeting the active ATP-binding pocket in Aurora B kinase with a K<sub>i</sub> of 0.36 nmol/L [39-41]. After pre-incubating Aurora B with the optimal inhibitor concentration, there was complete inhibition of enzymatic activity with 2.5 nM AZD1152-HQPA: no peak of the

phosphorylation product was observed in the electropherograms for up to 4 hrs (Fig. 3b; see ESM Figs. S16-17).

# Enzyme crosstalk with a mixture of substrates

After successfully monitoring enzyme reactions with one substrate, we proceeded to examine each enzyme reaction in more competitive environments. We monitored the methylation by G9a on a mixture of the FAM-labeled unphosphorylated (H3K9me<sub>0</sub>) and phosphorylated (H3K9me<sub>0</sub>S10p) histone peptides (Figure 4). As expected, the peak area of H3K9me<sub>0</sub>S10p did not change with the reaction lasting for 180 min, indicating the modified histone peptide was not methylated. On the other hand, the peak for the unmodified H3K9me<sub>0</sub> kept decreasing along with the increase of the peaks for H3K9me<sub>1-2</sub>. In addition, we subjected the mixture of unmethylated and dimethylated peptides to phosphorylation by Aurora B (Figure 5). The overall trend of rate difference on the unmodified and the methylated peptide was similar to the result presented in Fig. 3, which was obtained with a single substrate, although the overall reaction rate was slower due to degradation of the enzyme during storage. Still, successful monitoring of simultaneous reactions on substrate mixtures demonstrates the great value of our CE method in the study of enzyme crosstalk in an efficient manner, owing to its high resolution enabled by the high selectivity of the synthetic receptor for peptides carrying multiple PTMs.

# **Conclusion**

In this paper, we were able to monitor the activity of different enzyme reactions using host-assisted capillary electrophoresis. The combination of receptor selectivity and CE separation enhances the technique's efficacy in monitoring enzyme reactions. The use of a

permanent coating (LPA) on the inner capillary wall can improve the efficiency of separating multiply charged positive peptides, which were the targets in the enzyme activity crosstalk studies. The host-assisted CE method was able to monitor the reactions catalyzed by different PTM enzymes, such as G9a methyltransferase and Aurora B kinase, with individual substrates or competitive substrate mixtures (i.e., unmodified and modified peptide pairs) for effective analysis of the influence on enzyme activity by the presence of an antagonistic PTM. G9a methyltransferase was able to methylate H3K9me<sub>0</sub> while the presence of phosphorylation on the adjacent amino acid caused complete reduction in G9a activity overall. When monitoring the Aurora B kinase activity with CE, we observed successful phosphorylation of H3K9me<sub>0</sub> as well as a notable difference in activity with H3K9me<sub>2</sub>. In addition, we were able to detect the activity decrease in Aurora B kinase caused by a known inhibitor, AZD1152-HQPA. In the analysis of crosstalk events, host-assisted CE enables in situ analysis of the reaction mixture without the necessity of quenching the reaction; furthermore, it can simultaneously monitor the decrease in the substrate, the changes in the content of reaction intermediates, and the generation of the final product, providing rich information about the reaction process. In this regard, this technique should be valuable for the study of other possible antagonistic PTM pairs as well as synergistic PTMs in a complex biological environment.

**Acknowledgements** This work has been supported by the National Science Foundation award (CHE-1707347) to W.Z. and R.J.H.

Compliance with Ethical Standards All authors declare that this study does not include any experiments with human or animal subjects.

#### **Conflict of interest statement**

The authors declare that they have no conflict of interest.

# References

- 1. Mann M, Jensen ON. Proteomic analysis of post-translational modifications. Nat Biotechnol. 2003;21:255–61.
- 2. Fischle W, Wang Y, Allis CD. Histone and chromatin cross-talk. Curr Opin Cell Biol. 2003;172–83.
- 3. Vlaming H, Welsem T, Graaf EL, Ontoso D, Altelaar AM, San-Segundo PA, Heck AJ, Leeuwen F. Flexibility in crosstalk between H2B ubiquitination and H3 methylation in vivo . EMBO Rep. 2014;15:1220–1.
- Altaf M, Utley RT, Lacoste N, Tan S, Briggs SD, Côté J. Interplay of Chromatin Modifiers on a Short Basic Patch of Histone H4 Tail Defines the Boundary of Telomeric Heterochromatin. Mol Cell. 2007;28:1002–14.
- Zhang YY, Mei ZQ, Wu JW, Wang ZX. Enzymatic activity and substrate specificity of mitogen-activated protein kinase p38α in different phosphorylation states. J Biol Chem. 2008;283:26591–601.
- 6. Kim Y, Tanner KG, Denu JM. A continuous, nonradioactive assay for histone acetyltransferases. Anal Biochem. 2000;280:308–14.
- 7. Gowher H, Zhang X, Cheng X, Jeltsch A. Avidin plate assay system for enzymatic characterization of a histone lysine methyltransferase. Anal Biochem. 2005;342:287–91.
- 8. Cheung P, Tanner KG, Cheung WL, Sassone-corsi P, Denu JM, Allis CD. Synergistic

- Coupling of Histone H3 Phosphorylation and Acetylation in Response to Epidermal Growth Factor Stimulation. 2000;5:905–15.
- 9. Horiuchi KY, Eason MM, Ferry JJ, Planck JL, Walsh CP, Smith RF, Howitz KT, Ma H. Assay development for histone methyltransferases. Assay Drug Dev Technol. 2013;11:227–36.
- Scriba GKE, Belal F. Advances in Capillary Electrophoresis-Based Enzyme Assays.
   Chromatographia. 2015;78:947–70.
- 11. Dawson JF, Boland MP, Holmes CFB. A capillary electrophoresis-based assay for protein kinases and protein phosphatases using peptide substrates. Anal. Biochem. 220:340–5
- Lee KJ, Mwongela SM, Kottegoda S, Borland L, Nelson AR, Sims CE, Allbritton NL.
   Determination of sphingosine kinase activity for cellular signaling studies. Anal Chem.
   2008;80:1620–7.
- 13. Lee J, Perez L, Liu Y, Wang H, Hooley RJ, Zhong W. Separation of Methylated Histone Peptides via Host-Assisted Capillary Electrophoresis. Anal Chem. 2018;90:1881–8.
- Peck EM, Smith BD. Applications of Synthetic Receptors for Biomolecules. In: Smith BD, editor. Synthetic Receptors for Biomolecules: Design Principles and Applications.
   Cambridge: Royal Society of Chemistry; 2015. pp. 1–38.
- 15. Beshara CS, Jones CE, Daze KD, Lilgert BJ, Hof F. A simple calixarene recognizes post-translationally methylated lysine. ChemBioChem. 2010;11:63–6.
- Garnett GAE, Starke MJ, Shaurya A, Li J, Hof F. Supramolecular Affinity
   Chromatography for Methylation-Targeted Proteomics. Anal Chem. 2016;88:3697–3703.
- 17. Gamal-Eldin MA, MacArtney DH. Selective molecular recognition of methylated lysines and arginines by cucurbit[6]uril and cucurbit[7]uril in aqueous solution. Org Biomol

- Chem. 2013;11:488–95.
- 18. Liu Y, Perez L, Mettry M, Easley CJ, Hooley RJ, Zhong W. Self-Aggregating Deep Cavitand Acts as a Fluorescence Displacement Sensor for Lysine Methylation. J Am Chem Soc. 2016;138:10746–9.
- 19. Liu Y, Perez L, Gill AD, Mettry M, Li L, Wang Y, Hooley RJ, Zhong W. Site-Selective Sensing of Histone Methylation Enzyme Activity via an Arrayed Supramolecular Tandem Assay. J Am Chem Soc. 2017;139:10964–7.
- 20. Liu Y, Lee J, Perez L, Gill AD, Hooley RJ, Zhong W. Selective Sensing of Phosphorylated Peptides and Monitoring Kinase and Phosphatase Activity with a Supramolecular Tandem Assay. J Am Chem Soc. 2018;140:13869–77.
- Rea S, Eisenhaber F, O'Carroll D, Strahl BD, Sun Z-W, Schmid M, Opravil S, Mechtler K,
   Ponting CP, Allis CD, Jenuwein T. Regulation of chromatin structure by site-specific
   histone H3 methyltransferases. Nature. 2000;593–9.
- Duan Q, Chen H, Costa M, Dai W. Phosphorylation of H3S10 Blocks the Access of H3K9 by Specific Antibodies and Histone Methyltransferase IMPLICATION IN REGULATING CHROMATIN DYNAMICS AND EPIGENETIC INHERITANCE. J Biol Chem. 2008;283:33585–90.
- 23. Rathert P, Dhayalan A, Murakami M, Zhang X, Tamas R, Jurkowska R, Komatsu Y, Shinkai Y, Cheng X, Jeltsch A. Protein lysine methyltransferase G9a acts on non-histone targets. Nat Chem Biol. 2008;4:344–6.
- 24. Chin HG, Pradhan M, Estève PO, Patnaik D, Evans TC, Pradhan S. Sequence specificity and role of proximal amino acids of the histone H3 tail on catalysis of murine G9a lysine 9 histone H3 methyltransferase. Biochemistry. 2005;44:12998–13006.

- 25. Zhu G, Sun L, Dovichi NJ. Thermally-initiated free radical polymerization for reproducible production of stable linear polyacrylamide coated capillaries, and their application to proteomic analysis using capillary zone electrophoresis-mass spectrometry. Talanta. 2017;263:219–27.
- 26. Tachibana M, Sugimoto K, Nozaki M, Ueda J, Ohta T, Ohki M, Fukuda M, Takeda N, Niida H, Kato H, Shinkai Y. G9a histone methyltransferase plays a dominant role in euchromatic histone H3 lysine 9 methylation and is essential for early embryogenesis. 2002;3:1779–91.
- 27. Casciello F, Windloch K, Gannon F, Lee JS. Functional role of G9a histone methyltransferase in cancer. Front Immunol. 2015;6:3–9.
- 28. Shannon KB, Salmon ED. Chromosome dynamics: New light on Aurora B kinase function. Curr Biol. 2002;12:458–60.
- Muñoz-Barrera M, Monje-Casas F. Increased Aurora B activity causes continuous disruption of kinetochore-microtubule attachments and spindle instability. Proc Natl Acad Sci U S A. 2014;111:E3996–E4005.
- 30. Sugiyama K, Sugiura K, Hara T, Sugimoto K, Shima H, Honda K, Furukawa K, Yamashita S, Urano T. Aurora-B associated protein phosphatases as negative regulators of kinase activation. Oncogene. 2002;21:3103–11.
- 31. Beneito-Cambra M, Anres P, Vial J, Gareil P, Delaunay N. Stability and effectiveness of linear polyacrylamide capillary coating to suppress EOF in acidic media in the presence of surfactants, ionic liquids and organic modifiers. Talanta. 2016;150:546–52.
- 32. Isaacs L. Stimuli responsive systems constructed using cucurbit[ n ]uril-type molecular containers. Acc Chem Res. 2014;47:2052–62.

- 33. Perret F, Lazar AN, Coleman AW. Biochemistry of the para-sulfonato-calix[n]arenes. Chem Commun. 2006;2425–38.
- 34. Tachibana M, Sugimoto K, Fukushima T, Shinkai Y. SET Domain-containing Protein, G9a, is a Novel Lysine-preferring Mammalian Histone Methyltransferase with Hyperactivity and Specific Selectivity to Lysines 9 and 27 of Histone H3. J Biol Chem. 2001;276:25309–17.
- 35. Osipovich O, Milley R, Meade A, Tachibana M, Shinkai Y, Krangel MS, Oltz EM.

  Targeted inhibition of V ( D ) J recombination by a histone methyltransferase. Nat

  Immunol. 2004;5:309–16.
- 36. Collins RE, Tachibana M, Tamaru H, Smith KM, Jia D, Zhang X, Selker EU, Shinkai Y, Cheng X. In vitro and in vivo analyses of a Phe/Tyr switch controlling product specificity of histone lysine methyltransferases. J Biol Chem. 2005;280:5563–70.
- 37. Patnaik D, Hang GC, Estève PO, Benner J, Jacobsen SE, Pradhan S. Substrate specificity and kinetic mechanism of mammalian G9a histone H3 methyltransferase. J Biol Chem. 2004;279:53248–58.
- 38. Cohen SL, Chait BT. Influence of matrix solution conditions on the MALDI-MS analysis of peptides and proteins. Anal Chem. 1996;68:31–7.
- 39. Sessa F, Villa F. Structure of Aurora B-INCENP in complex with barasertib reveals a potential transinhibitory mechanism. Acta Crystallogr F Struct Biol Commun. 2014;70:294–8.
- 40. Tang A, Gao K, Chu L, Zhang R, Yang J, Zheng J. Aurora kinases: novel therapy targets in cancers. Oncotarget. 2017;8:23937–54.
- 41. Wilkinson RW, Odedra R, Heaton SP, Wedge SR, Keen NJ, Crafter C, Foster JR, Brady

MC, Bigley A, Brown E, Byth KF, Barrass NC, Mundt KE, Foote KM, Heron NM, Jung FH, Mortlock AA, Boyle FT, Green S. Cancer Therapy: Preclinical AZD1152, a Selective Inhibitor of Aurora B Kinase, Inhibits Human umor Xenograft Growth by Inducing Apoptosis. Clin Cancer Res. 2007;13:3682–9.

#### **Figure Captions**

**Fig. 1 a** Separation of FAM-labeled H3K9me<sub>0,2</sub> peptides in 0 μM host, 0.5 μM CX4, 0.5 μM CX6, and 0.5 μM CB7 in 10 mM phosphate buffer, pH 7.4. **b** Separation of FAM-labeled H3K9me<sub>0,2</sub>S10p peptides in 0 μM host, 10 μM CX4, 10 μM CX6, and 10 μM CB7 in 10 mM phosphate buffer, pH 7.4. Separation of FAM-labeled H3K9me<sub>0,2</sub> peptides (**c**) or FAM-labeled H3K9me<sub>0,2</sub>S10p peptides (**d**) in 10 mM phosphate buffer and 10 mM tris buffer at pH 7.4. Electric field strength = 662 V/cm

**Fig. 2 a** Separation of the FAM-labeled H3K9me<sub>0</sub> substrate and products, H3K9me<sub>1-3</sub>, during a G9a methyltransferase reaction over time. **b** Progression of the G9a reaction with FAM-labeled H3K9me<sub>0</sub>S10p as a substrate over time. **c** Percent peak area (FAM-labeled H3K9me<sub>x</sub>; x=0,1,2,3; peak area over the total peak area) versus time using electropherogram data. **d** % peak area (FAM-labeled H3K9me<sub>x</sub>S10p; x=0,1,2,3; peak area over the total peak area) versus time using electropherogram data. Reaction conditions: [peptide] = 10 μM, [G9a] = 0.25 μM, [SAM] = 500 μM, [Mg<sup>2+</sup>] = 0.1 mM in 20 mM tris pH 9.0 at room temperature. Separation buffer = 2 μM (**a**) or 10 μM (**b**) CX6 in 10 mM phosphate buffer, pH 7.4. Electric field strength = 662 V/cm

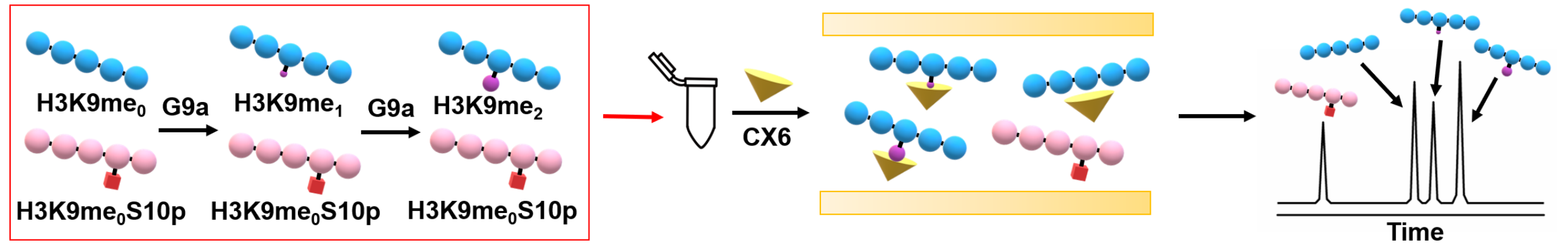
**Fig. 3 a** % peak area (FAM-labeled H3K9me<sub>x</sub>S10p, x=0,2 peak area over the total peak area) versus time using electropherogram data from the Aurora B kinase reaction. **b** % peak area (FAM-labeled H3K9me<sub>0</sub>S10p peak area over the total peak area) versus time in the presence and absence of the AZD1152-HQPA inhibitor during an Aurora B kinase reaction. Reaction conditions: [peptide] = 10 μM, [ATP] = 20 μM, [Mg<sup>2+</sup>] = 0.1 mM, [Aurora B] = 0.005 μg/μL (**a**) or 0.01 μg/μL (**b**), [AZD1152-HQPA] = 0 or 2.5 nM in 20 mM tris pH 7.4 at room temperature

**Fig. 4 a** Schematic for the separation of unphosphorylated and phosphorylated peptides as well as their products during a G9a methyltransferase reaction over time. **b** Separation of FAM-labeled H3K9me<sub>0</sub> and H3K9me<sub>0</sub>S10p substrates and their products during a G9a reaction over time. Separation buffer = 2 μM CX6 in 10 mM phosphate buffer, pH 7.4. Electric field strength = 662 V/cm. **c** % peak area (FAM-labeled H3K9me<sub>x</sub>; x=0,1,2; peak area over the total peak area) versus time for the G9a substrate mixture reaction. **d** % peak area (FAM-labeled H3K9me<sub>x</sub>S10p; x=0,1,2; peak area over the total peak area) versus time for the G9a substrate mixture reaction. Reaction conditions: [H3K9me<sub>0</sub>] = 10 μM, [H3K9me<sub>0</sub>S10p] = 30 μM, [G9a] = 0.25 μM, [SAM] = 500 μM, [Mg<sup>2+</sup>] = 0.1 mM in 20 mM tris pH 9.0 at room temperature

**Fig. 5 a** Schematic for the separation of unmethylated and methylated peptides as well as their products during an Aurora B kinase reaction over time. **b** Separation of FAM-labeled H3K9me<sub>0</sub> and H3K9me<sub>2</sub> substrates and their products during an Aurora B reaction over time. Separation buffer = 2 μM CX6 in 10 mM phosphate buffer, pH 7.4. Electric field strength = 662 V/cm. **c** % peak area (FAM-labeled H3K9me<sub>x</sub>S10p; x=0,2; peak over the total peak area) versus time for the Aurora B kinase substrate mixture reaction. Reaction conditions: [peptide] = 10 μM, [ATP] = 20 μM, [Mg<sup>2+</sup>] = 0.1 mM, [Aurora B] = 0.005 μg/μL in 20 mM tris pH 7.4 at room temperature

# Graphical Abstract

# **G9a Methyltransferase Reaction**



# **Aurora B Kinase Reaction**

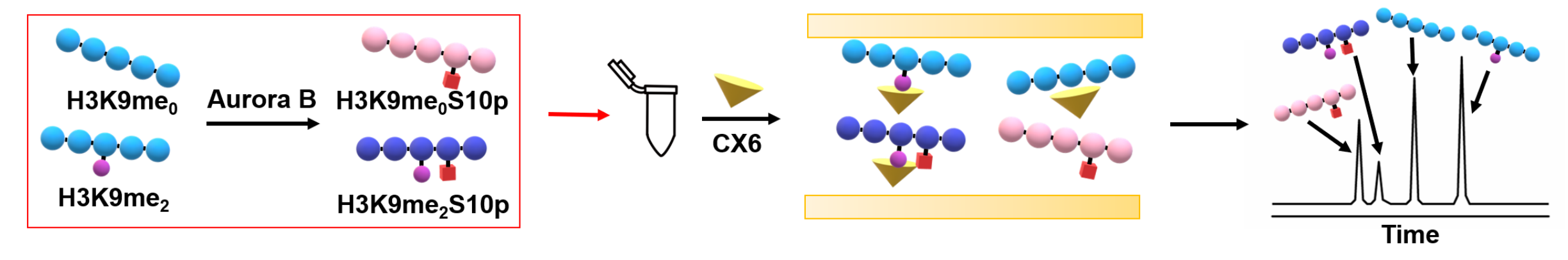


Fig. 1

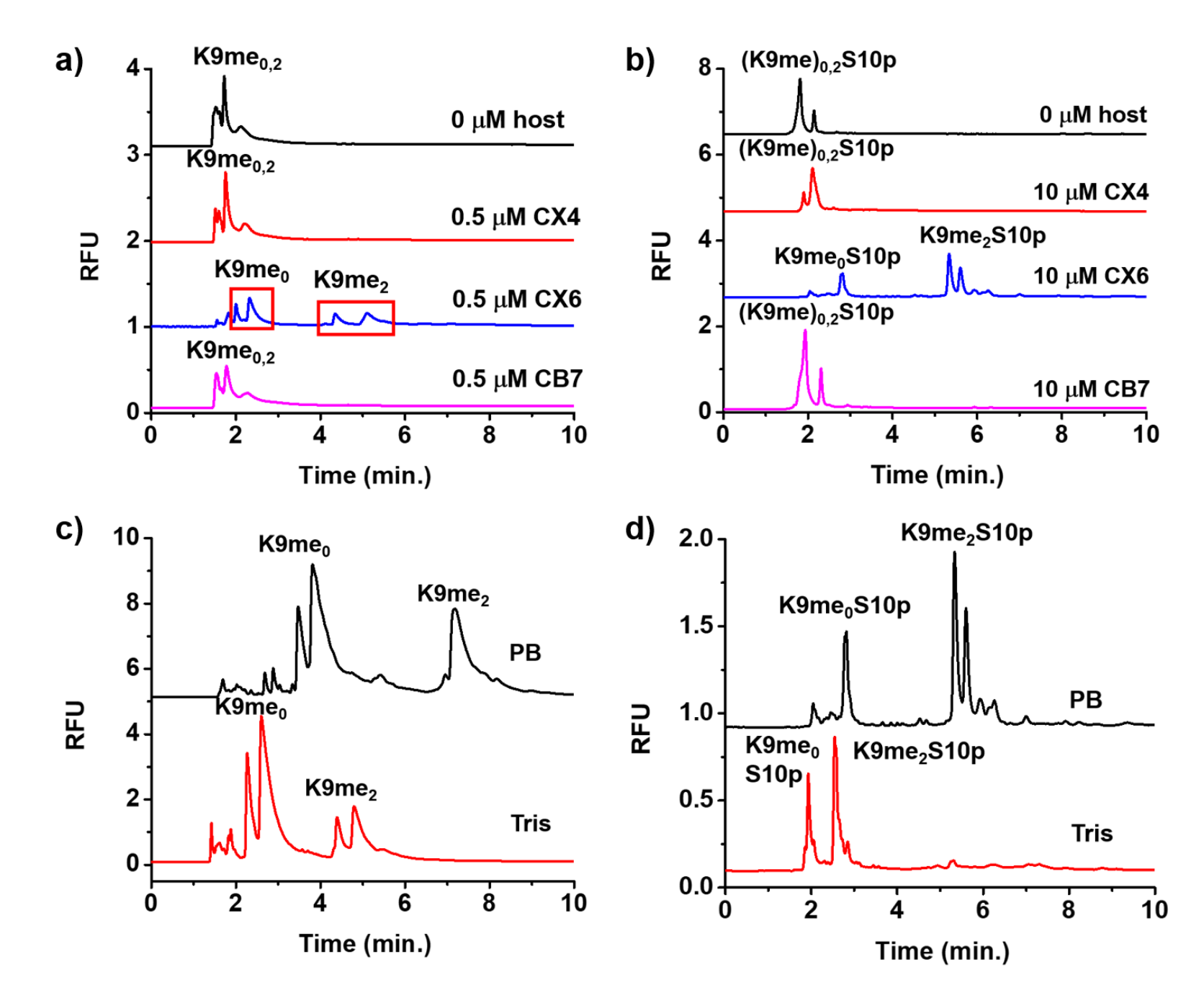


Fig. 2

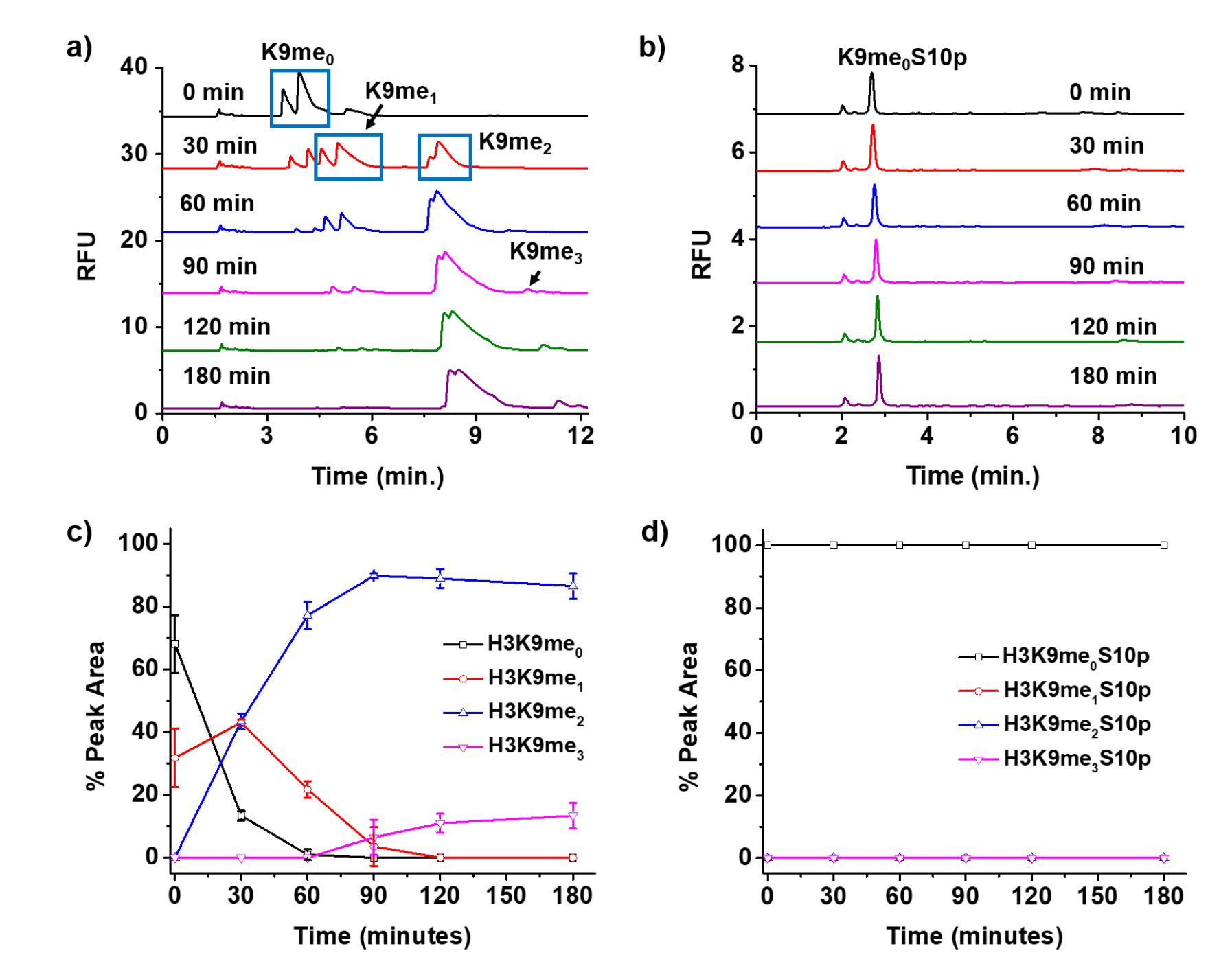


Fig. 3

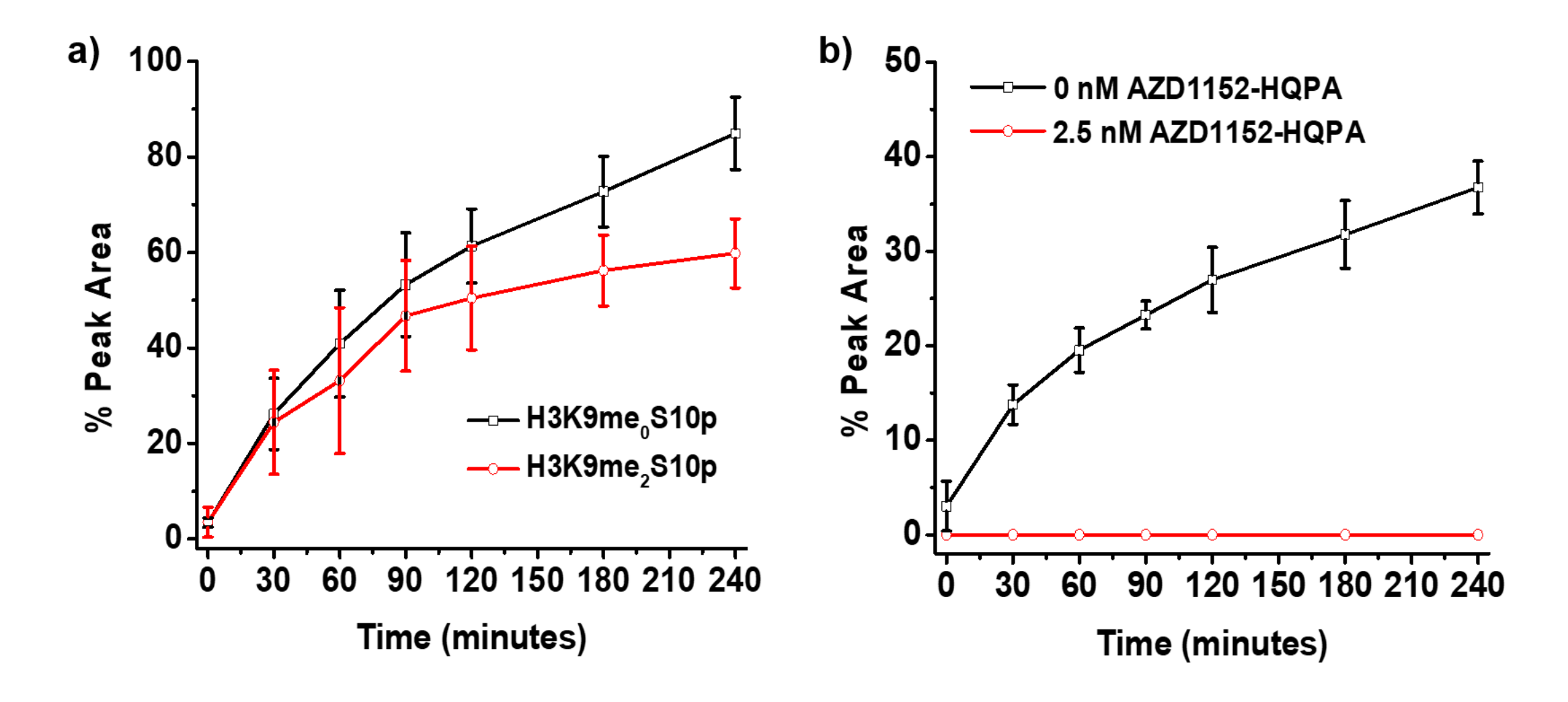


Fig. 4

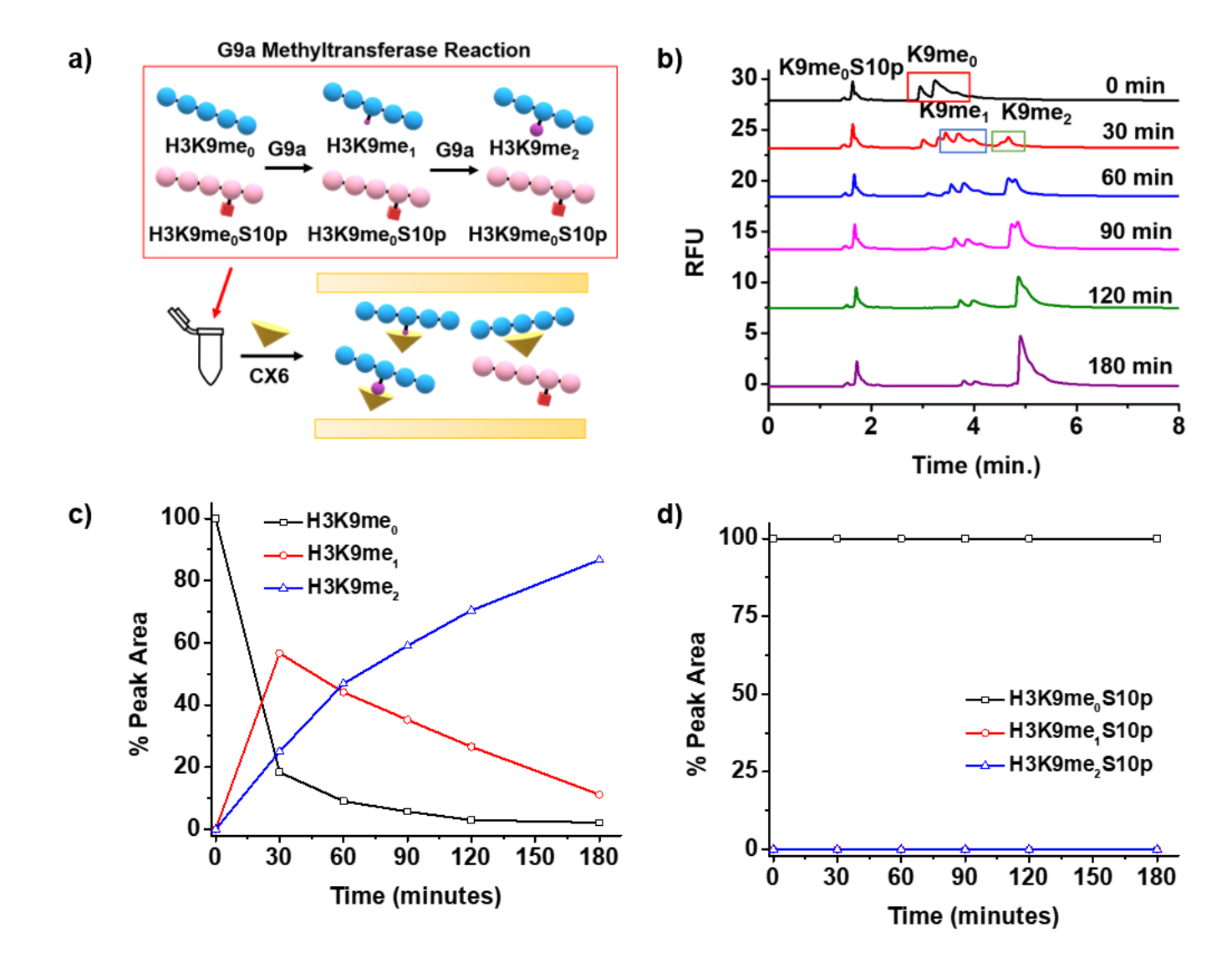
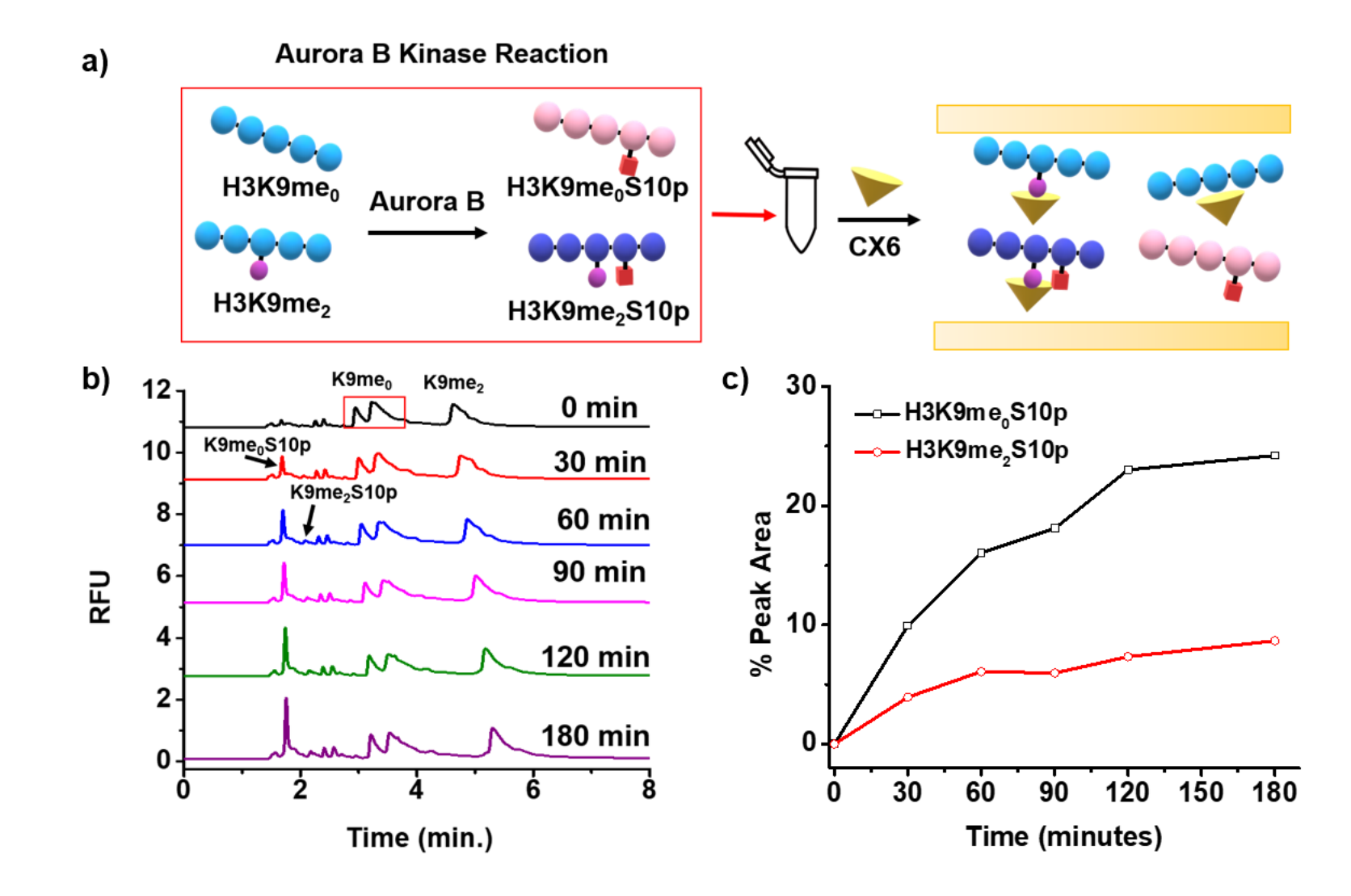


Fig. 5



Analytical and Bioanalytical Chemist	Analy	tical	and	Bioana	lytical	Chei	nistry
--------------------------------------	-------	-------	-----	--------	---------	------	--------

**Electronic Supplementary Material** 

Monitoring the Crosstalk between Methylation and Phosphorylation on Histone Peptides with Host-Assisted Capillary Electrophoresis

Jiwon Lee, Junyi Chen, Priyanka Sarkar, Min Xue, Richard J. Hooley, Wenwan Zhong

Reagents and Chemicals. All samples and separation buffers were made using ultrapure water (18 MΩ) from a Direct-Q Water Purification System (Millipore Sigma, Billerica, MA).  $\alpha$ -Lactalbumin, lysozyme, cytochrome c, hemoglobin, 4-tetrasulfonatocalix[4]arene, cucurbit[7]uril hydrate, 3-(trimethoxysilyl)propyl methacrylate, acrylamide, ammonium persulfate,  $\alpha$ -cyano-4-hydroxycinnamic acid ( $\alpha$ -CHCA), adenosine 5'-triphosphate disodium salt hydrate, s-(5'-adenosyl)-L-methionine (SAM) chloride dihydrochloride, and magnesium chloride hexahydrate were purchased from Sigma-Aldrich (St. Louis, MO). 4-Hexasulfonatocalix[6]arene hydrate was purchased from Alfa Aesar (Tewksbury, MA). 5(6)-Carboxyfluorescein was purchased from ACROS Organics (Morris Plains, NJ). All 9-fluorenylmethyloxycarbonyl-protected amino acids were purchased from AAPPTec (Louisville, KY) except for Fmoc-N-ε-dimethyl-L-lysine hydrochloride (ChemPep Inc., Wellington, FL) and N- $\alpha$ -Fmoc-O-benzyl-L-phosphoserine (Millipore Sigma, Billerica, MA). Lyophilized, non-labeled histone K9 peptides were purchased from AnaSpec, Inc. (Fremont, CA). The sequence is ARTKQTAR-K(me<sub>x</sub>)-STGGKAPRKQLA (x = 0, 1, 2, 3).

**Separation Performance on Linear Polyacrylamide-Coated Capillary.** Non-fluorescent peptides were separated on an Agilent 7100 CE system with a UV-visible diode-array detector. Data were acquired via ChemStation (Agilent Technologies, Santa Clara, CA). Samples were introduced into an LPA-coated capillary (50 μm inner diameter, 365 μm outer diameter, with an effective length of 26.5 cm) with a 50 mbar injection for 5 s. Separation was driven by an electric field of 571 V/cm with positive polarity.

Synthesis and Purification of 11-Amino Acid Peptides. Amino acids were sequenced using Peptide Synthesizer CSBio CS336H on FMOC-rink amide MBHA resin. UHPLC was performed on a Dionex system: UltiMate 3000 pump and variable wavelength detector. A C-18 reversed phase column (5 μm diameter, 100 Å, 250 × 21.2 mm) was used. Solvent A was 0.1% TFA in water and solvent B was 0.1% TFA in acetonitrile when using the gradient solvent system: solvent B (0-40%) in solvent A from the 0- to 7-minute mark at a flow rate of 3.0 mL/ min, solvent B (40–75%) in solvent A from 7- to 30-minute mark at a flow rate of 8.0 mL/min, and solvent B (75-100%) in solvent A from the 30- to 40-minute mark at a flow rate of 15.0 mL/min. Data acquisition was completed on the Chromeleon 7.2 Chromatography Data System software. Fractions were collected with a Dionex UltiMate 3000 Automated Fraction Collector. The mass of each peptide was determined using MALDI-TOF MS. 0.5 μL of each fraction and 2.5 μL of matrix (saturated α-CHCA in a 1:1 ratio of acetonitrile and 0.1% formic acid in water) were mixed before spotting each sample on a stainless steel Opti-TOF 96-target plate. Each spot was left to dry before introduction into the mass spectrometer. MS spectra were acquired in a positive reflector mode using the AB Sciex 5800 TOF/TOF proteomics analyzer. Solvent from the peptide fractions was then removed, and samples were lyophilized.

MALDI-TOF MS Analysis. The enzymatic assays were performed as described above. Aliquots were removed and deactivated by direct addition to the matrix solution. The matrix solution was prepared to form a saturated solution of α-cyano-4-hydroxycinnamic acid (CHCA) in a 1:1 ratio of acetonitrile and 0.1% formic acid. A 1:1 ratio of matrix and sample was spotted on a stainless steel Opti-TOF 96-target plate and left to dry before inserting into the mass spectrometer. MS

spectra were acquired in positive reflector mode using the AB Sciex 5800 TOF/TOF proteomics analyzer with laser irradiation at a repetition frequency of 1000 Hz.

#### **Calculations**

The tailing factor (t) was calculated with the following equation:

$$t = \frac{w_{5.0}}{t_w \cdot 2}$$
 Equation S1

where  $w_{5.0}$  = peak width at 5% of peak height (min.) and  $t_w$  = distance (min.) between peak front and peak center.

In order to assess the separation performance, the resolution (R) was calculated with the following equation:

$$R = \frac{2 (t_2 - t_1)}{w_1 + w_2}$$
 Equation S2

where  $t_1$  and  $t_2$  are the migration times of peaks 1 and 2, respectively. Furthermore,  $w_1$  and  $w_2$  are the base peak widths of peaks 1 and 2, respectively.

Table S1 Peptide sequences of FAM-labeled H3 (1-11) peptides

Peptide	Sequence
H3K9me <sub>0</sub>	FAM-ARTKQTARKST
H3K9me <sub>2</sub>	FAM-ARTKQTAR-K(me <sub>2</sub> )-ST
$H3K9me_0S10p$	FAM-ARTKQTARK-pS-T
H3K9me <sub>2</sub> S10p	FAM-ARTKQTAR-K(me <sub>2</sub> )-pS-T

**Table S2** Average migration times, peak areas, and tailing factors (triplicate measurements) for standard proteins in linear polyacrylamide (LPA)-coated capillaries

	Migration Time (min)		Peak Area		Tailing Factor	
Protein			(mAU x r	min)		
	Average	RSD (%)	Average	RSD (%)	Average	RSD (%)
Cytochrome c	3.72	1.2	62.9	0.6	4.1	0.3
Lysozyme	4.11	1.2	154.8	2.2	2.4	0.2
α-lactalbumin	4.73	1.3	77.8	1.6	1.9	0.1
Hemoglobin	5.28	1.5	39.0	6.2	2.2	0.1

**Table S3** Average migration times and peak areas (triplicate measurements) for 21-amino acid unlabeled H3K9me<sub>0-3</sub> peptides in LPA-coated capillaries

Peptide	Migration Time (min)		Peak Area (mAU x min)	
	Average	RSD (%)	Average	RSD (%)
H3K9me <sub>0</sub>	6.67	0.1	167.8	8.6
H3K9me <sub>1</sub>	7.79	0.1	187.7	8.3
H3K9me <sub>2</sub>	9.15	0.2	216.3	8.3
H3K9me <sub>3</sub>	10.14	0.2	350.5	28.7

**Table S4** Resolution of FAM-labeled H3 (1-11) peptide peaks in phosphate and tris buffers. For resolution calculation when isomer peaks (originated from the isomeric FAM) were present, the later migrating isomer peak of the first peptide and the earlier migrating isomer peak of the second peptide were used.

Peptide Pair	Phosphate	Tris
H3K9me <sub>0,2</sub>	3.4	2.4
H3K9me <sub>0,2</sub> S10p	5.1	1.0

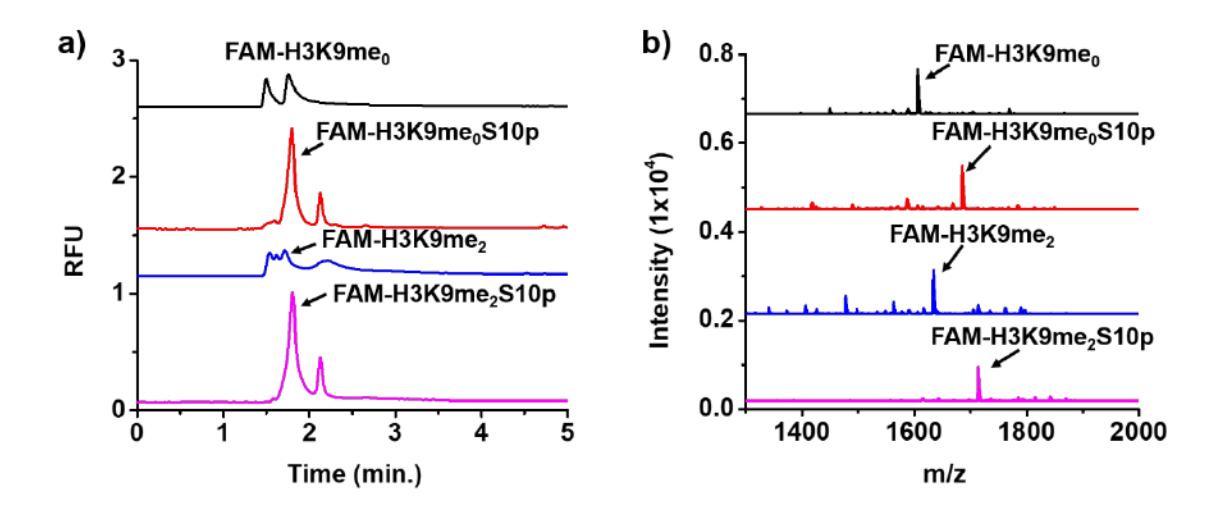


Fig. S1 Purity of each peptide shown in (a) a CE electropherogram and (b) a MALDI spectrum

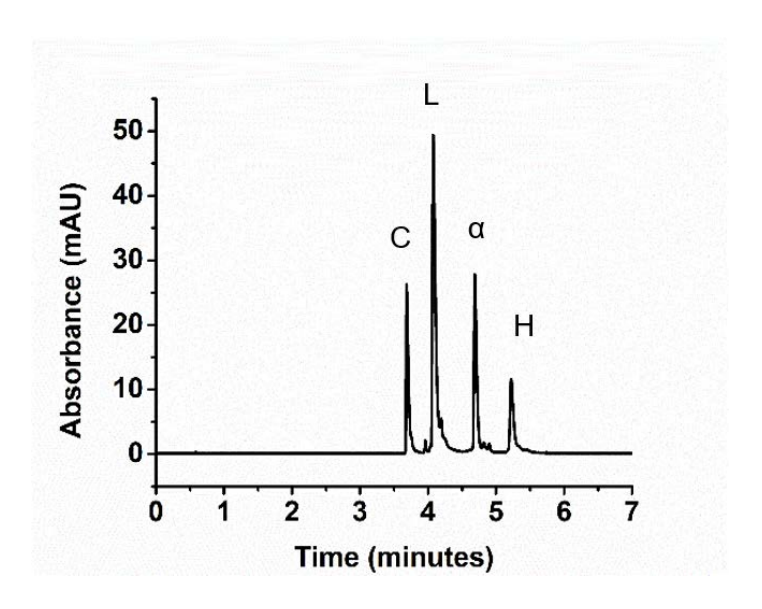
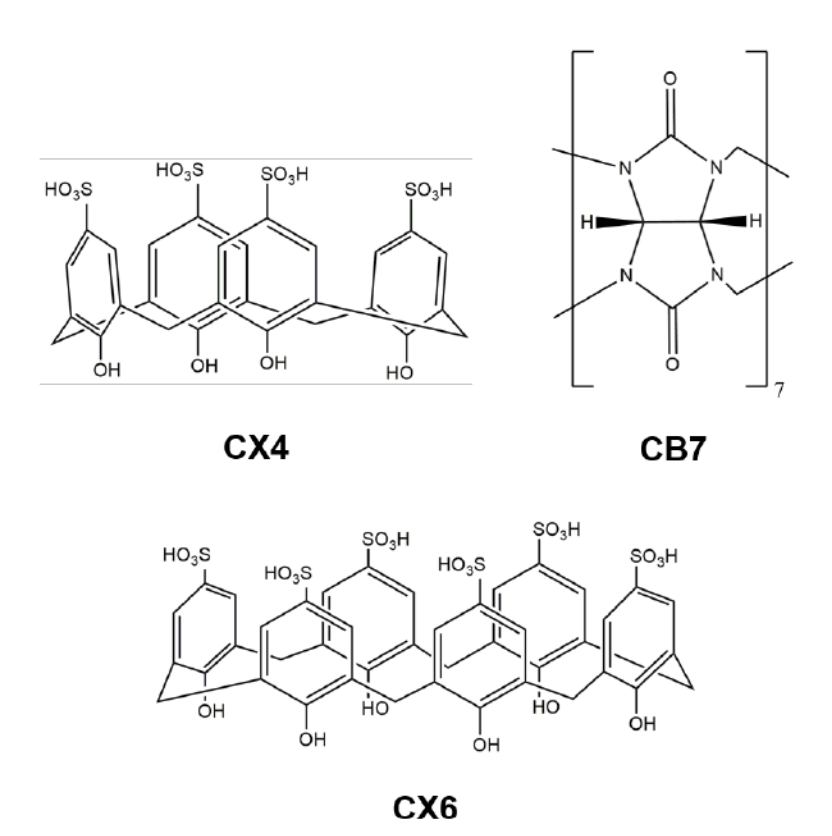
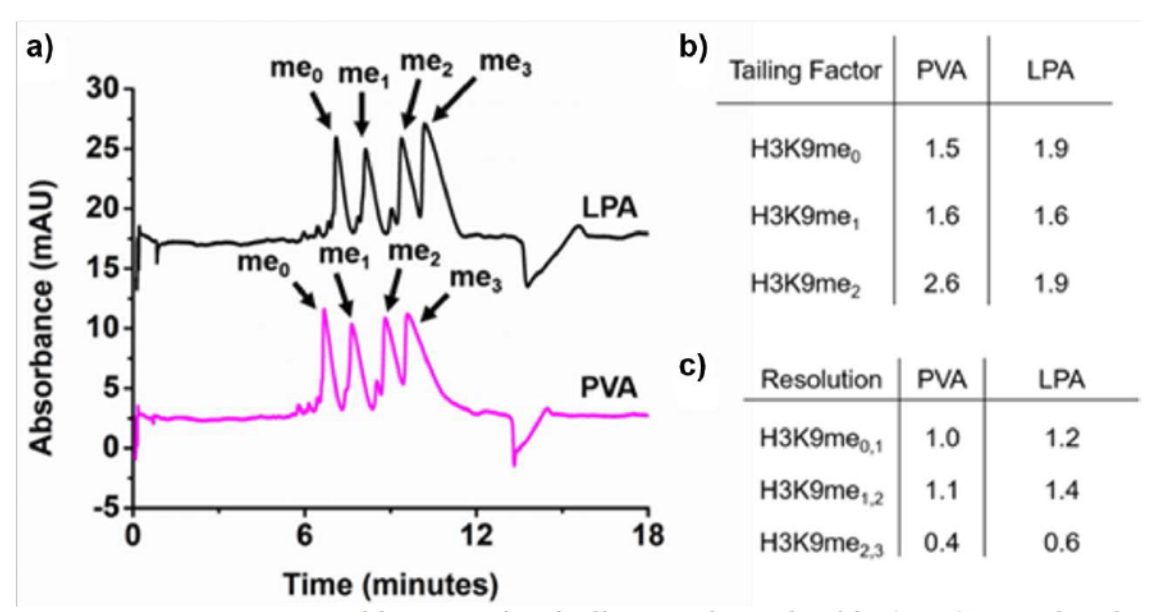


Fig. S2 Separation of a standard protein mixture in an LPA-coated capillary. C = cytochrome c, L = lysozyme,  $\alpha = \alpha$ -lactalbumin, and H = hemoglobin. [Protein] = 0.25 mg/mL, background electrolyte = 50 mM phosphate buffer, pH 2.8, electric field strength = 429 V/cm



**Fig. S3** Structures of synthetic receptors: 4-tetrasulfonatocalix[4]arene (CX4), 4-hexasulfonatocalix[6]arene (CX6), and cucurbit[7]uril (CB7)



**Fig. S4 a** H3K9me<sub>0-3</sub> peptide separation in linear polyacrylamide (LPA)-coated and polyvinyl alcohol (PVA)-coated capillaries. Values for the tailing factor, t, (**b**) and resolution, R, (**c**) for 21-amino acid unlabeled H3K9me<sub>0-3</sub> peptides in PVA- and LPA-coated capillaries. t was calculated using equation S1 while R was calculated using equation S2. The sequence of the peptide is ARTKQTAR-K(me<sub>x</sub>)-STGGKAPRKQLA (x = 0, 1, 2, 3). [peptide] = 50  $\mu$ M, background electrolyte = 50  $\mu$ M CX4 in 50 mM phosphate buffer, pH 2.8, electric field strength = 571 V/cm with added 5 mbar of pressure

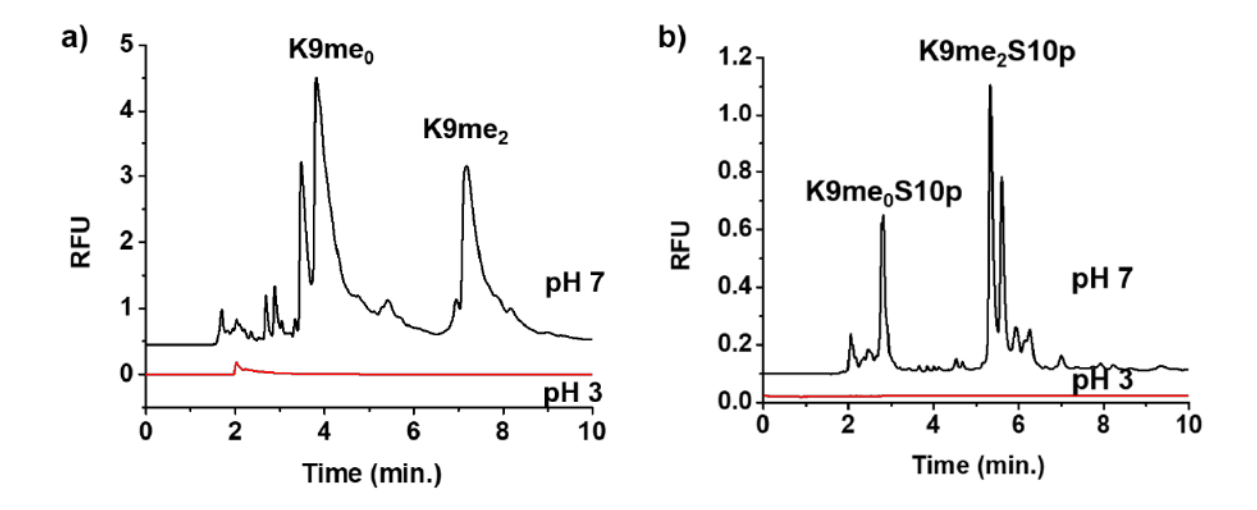


**Fig. S5** Separation of FAM-labeled H3K9me<sub>0,2</sub> peptides (**a**) and FAM-labeled H3K9me<sub>0,2</sub>S10p peptides (**b**). Separation buffer = 2  $\mu$ M (**a**) or 10  $\mu$ M (**b**) CX6 in 10 mM phosphate buffer, pH 3.0 or 7.4 (as noted in the figure). Electric field strength = 662 V/cm

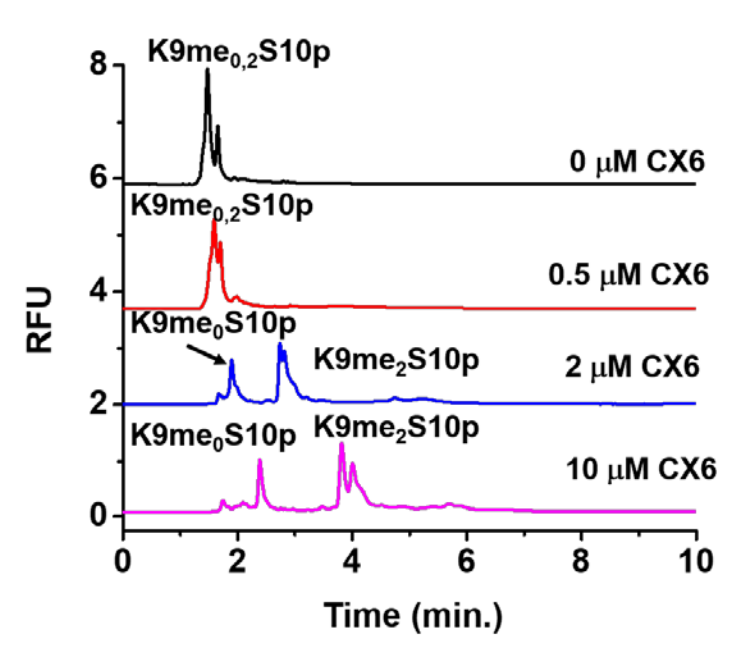


**Fig. S3** Optimization of FAM-labeled H3K9me<sub>0,2</sub>S10p separation in various concentrations of CX6, ranging from 0  $\mu$ M to 10  $\mu$ M CX6 in 10 mM phosphate buffer, pH 7.4. Electric field strength = 662 V/cm

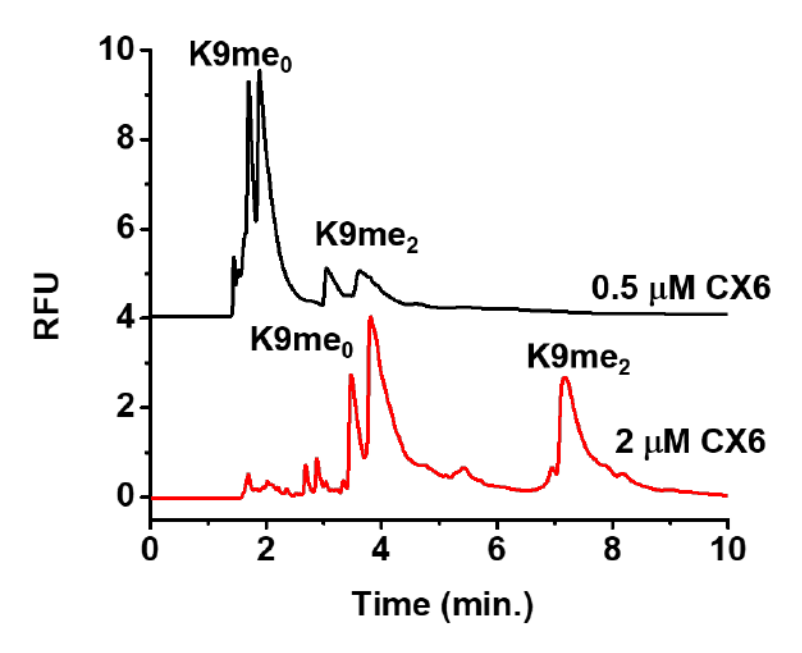


**Fig. S4** Comparison of FAM-labeled H3K9me<sub>0,2</sub> peptide separation in 0.5  $\mu$ M vs. 2  $\mu$ M CX6 in 10 mM phosphate buffer, pH 7.4. Electric field strength = 662 V/cm

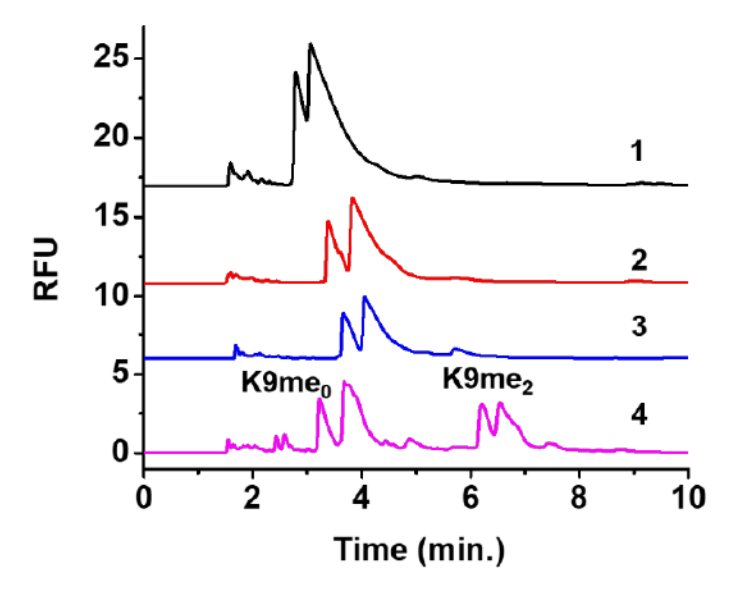


**Fig. S5** Controls for G9a reaction with FAM-labeled H3K9me<sub>0</sub>. Trace  $1-10~\mu M$  H3K9me<sub>0</sub> peptide; trace  $2-10~\mu M$  H3K9me<sub>0</sub> peptide with cofactors (500 μM SAM, 0.1 mM Mg<sup>2+</sup>); trace 3 - 10 μM H3K9me<sub>0</sub> peptide with cofactors (500 μM SAM, 0.1 mM Mg<sup>2+</sup>) and 0.25 μM deactivated G9a; trace  $4-H3K9me_2$  spiked into reaction of  $10~\mu M$  H3K9me<sub>0</sub> peptide with cofactors (500 μM SAM, 0.1 mM Mg<sup>2+</sup>) and 0.25 μM deactivated G9a. Separation buffer = 2 μM CX6 in 10 mM phosphate buffer, pH 7.4. Electric field strength = 662 V/cm

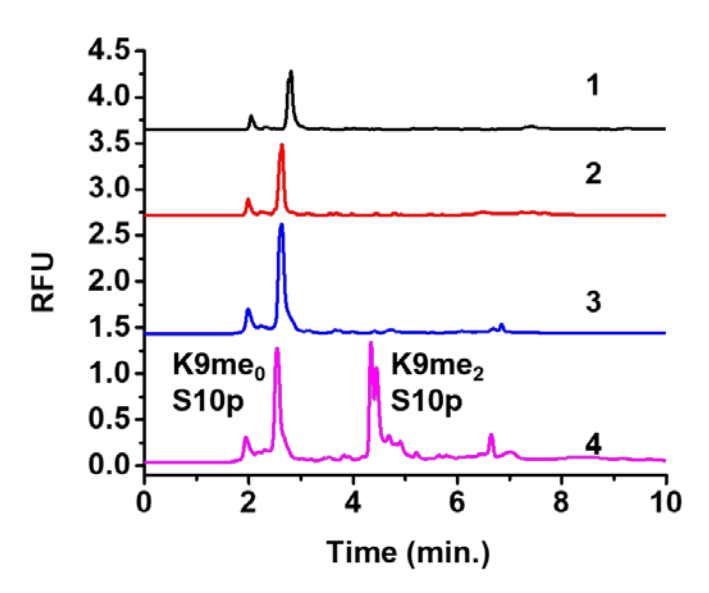


**Fig. S6** Controls for G9a reaction with FAM-labeled H3K9me<sub>0</sub>S10p. Trace 1 – 10 μM H3K9me<sub>0</sub>S10p peptide; trace 2 – 10 μM H3K9me<sub>0</sub>S10p peptide with cofactors (500 μM SAM, 0.1 mM Mg<sup>2+</sup>); trace 3 - H3K9me<sub>0</sub>S10p peptide with cofactors (500 μM SAM, 0.1 mM Mg<sup>2+</sup>) and deactivated 0.25 μM G9a; trace 4 - H3K9me<sub>2</sub>S10p spiked into reaction of H3K9me<sub>0</sub>S10p peptide with cofactors (500 μM SAM, 0.1 mM Mg<sup>2+</sup>) and deactivated 0.25 μM G9a. Separation buffer = 10 μM CX6 in 10 mM phosphate buffer, pH 7.4. Electric field strength = 662 V/cm

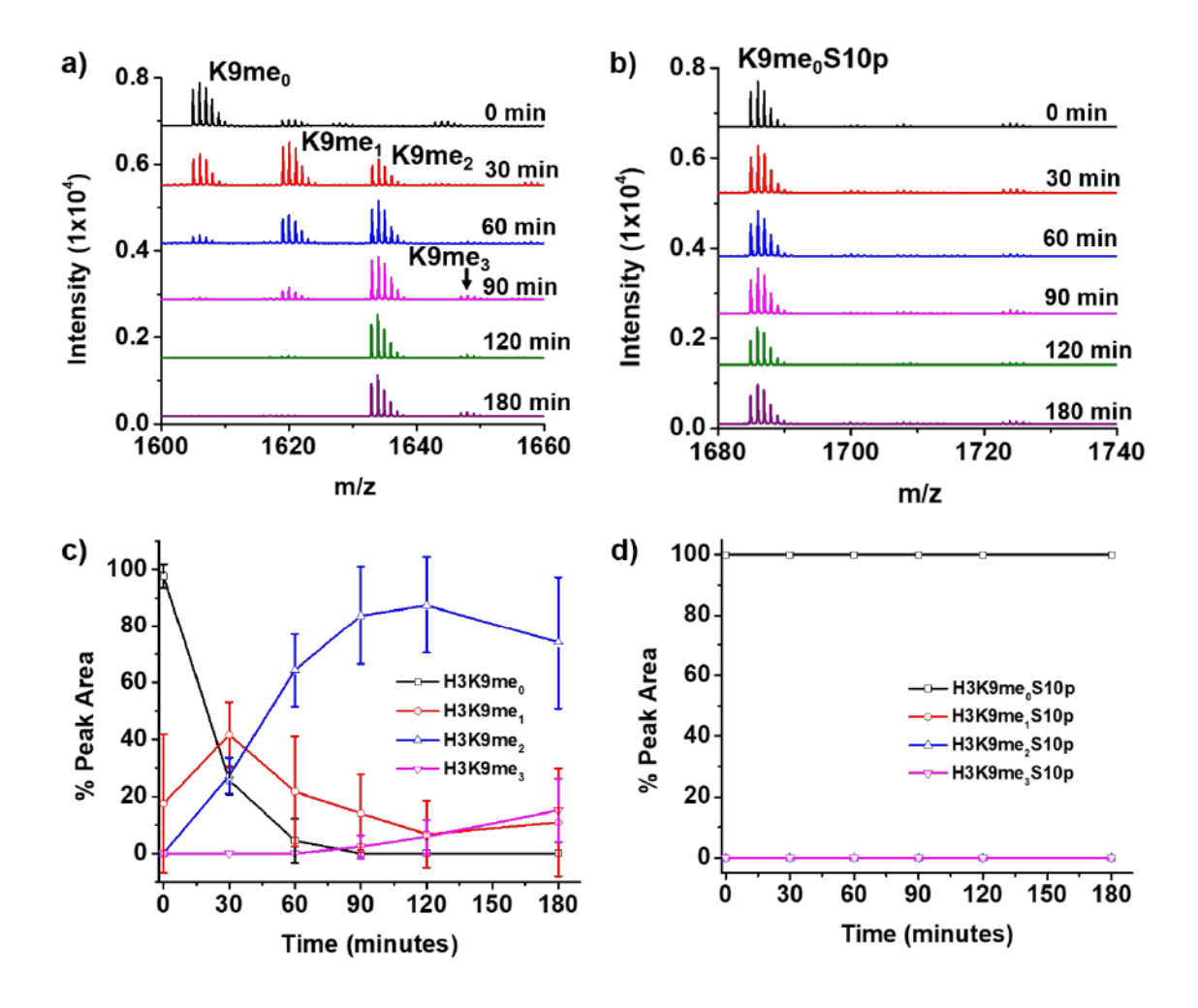


**Fig. S7 a** MALDI-TOF/TOF spectra with FAM-labeled H3K9me<sub>0</sub> substrate and products,FAM-labeled H3K9me<sub>1-3</sub>, during a G9a methyltransferase reaction over time. **b** MALDI-TOF/TOF spectra for progression of G9a methyltransferase reaction with FAM-labeled H3K9me<sub>0</sub>S10p as a substrate over time. **c** % peak area (FAM-labeled H3K9me<sub>x</sub>; x=0,1,2,3; peptide peak over the total peak area) versus time using MALDI-TOF/TOF data. **d** % peak area (FAM-labeled H3K9me<sub>x</sub>S10p; x=0,1,2,3; peptide peak over the total peak area) versus time using MALDI-TOF/TOF data. Reaction conditions: [peptide] = 10 μM, [G9a] = 0.25 μM, [SAM] = 500 μM, [Mg<sup>2+</sup>] = 0.1 mM in 20 mM tris pH 9.0 at room temperature

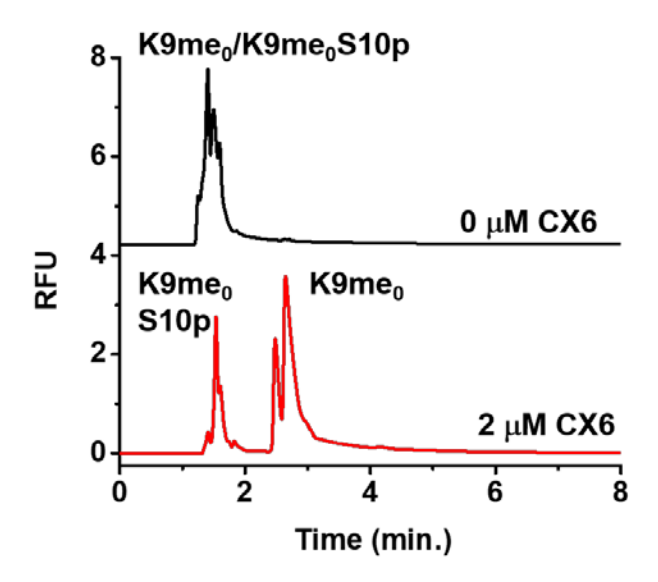
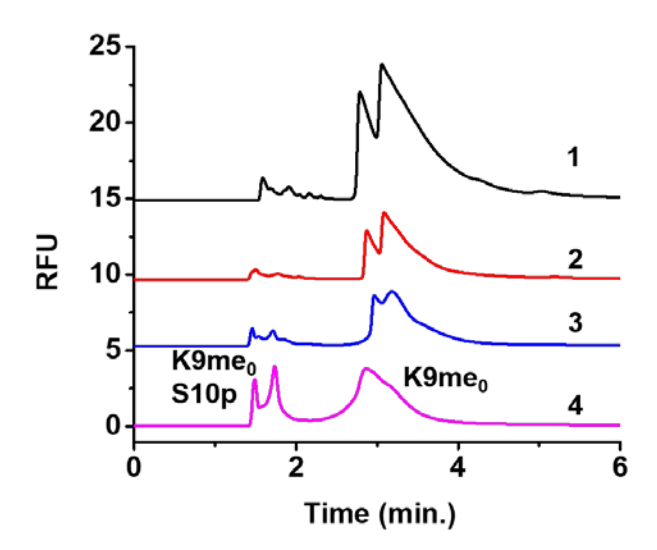
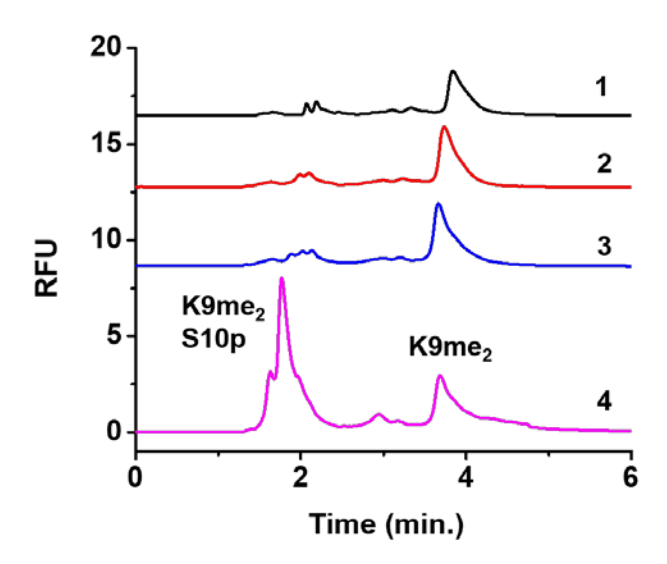


Fig. S8 Comparison of FAM-labeled H3K9me $_0$  and FAM-labeled H3K9me $_0$ S10p separation in 0  $\mu$ M and 2  $\mu$ M CX6 in 10 mM phosphate buffer, pH 7.4. Electric field strength = 662 V/cm



**Fig. S9** Controls for Aurora B kinase reaction with FAM-labeled H3K9me<sub>0</sub>. Trace  $1-10~\mu M$  H3K9me<sub>0</sub> peptide; trace  $2-10~\mu M$  H3K9me<sub>0</sub> peptide with cofactors (20  $\mu M$  ATP, 0.1 mM Mg<sup>2+</sup>); trace  $3-10~\mu M$  H3K9me<sub>0</sub> peptide with cofactors (20  $\mu M$  ATP, 0.1 mM Mg<sup>2+</sup>) and 0.005  $\mu g/\mu L$  deactivated Aurora B kinase; trace  $4-H3K9me_0S10p$  spiked into reaction of  $10~\mu M$  H3K9me<sub>0</sub> peptide with cofactors (20  $\mu M$  ATP, 0.1 mM Mg<sup>2+</sup>) and 0.005  $\mu g/\mu L$  deactivated Aurora B kinase. Separation buffer =  $2~\mu M$  CX6 in 10~m M phosphate buffer, pH 7.4. Electric field strength = 662~V/cm



**Fig. S10** Controls for Aurora B kinase reaction with FAM-labeled H3K9me<sub>2</sub>. Trace  $1-10~\mu M$  H3K9me<sub>2</sub> peptide; trace  $2-10~\mu M$  H3K9me<sub>2</sub> peptide with cofactors (20  $\mu M$  ATP, 0.1 mM Mg<sup>2+</sup>); trace  $3-10~\mu M$  H3K9me<sub>2</sub> peptide with cofactors (20  $\mu M$  ATP, 0.1 mM Mg<sup>2+</sup>) and 0.005  $\mu g/\mu L$  deactivated Aurora B kinase; trace  $4-H3K9me_2S10p$  spiked into reaction of  $10~\mu M$  H3K9me<sub>2</sub> peptide with cofactors (20  $\mu M$  ATP, 0.1 mM Mg<sup>2+</sup>) and 0.005  $\mu g/\mu L$  deactivated Aurora B kinase. Separation buffer =  $2~\mu M$  CX6 in 10~m M phosphate buffer, pH 7.4. Electric field strength = 662~V/cm

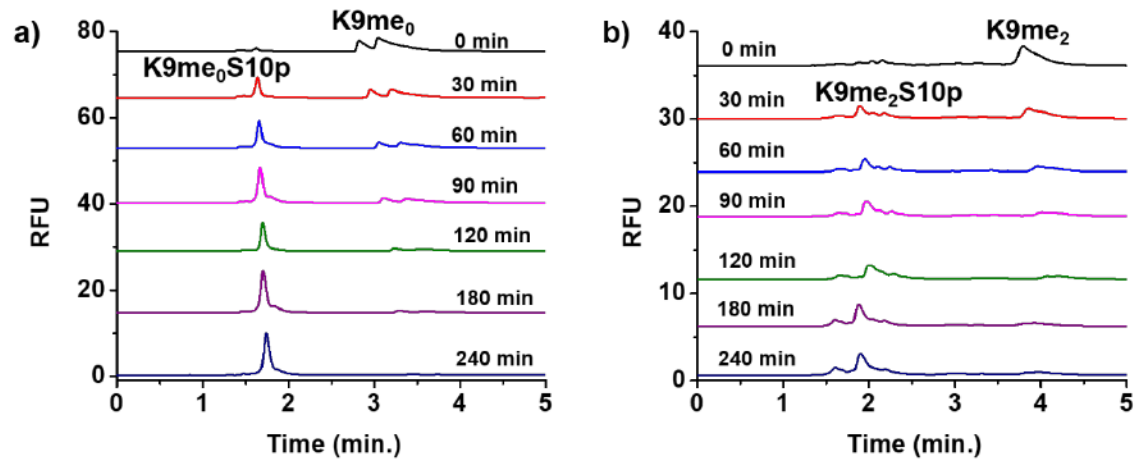


**Fig. S14 a** Separation of FAM-labeled H3K9me<sub>0</sub> substrate and FAM-labeled H3K9me<sub>0</sub>S10p product during an Aurora B kinase reaction over time. **b** Separation of FAM-labeled H3K9me<sub>2</sub> substrate and FAM-labeled H3K9me<sub>2</sub>S10p product during an Aurora B kinase reaction over time. Reaction conditions: [peptide] = 10 μM, [ATP] = 20 μM, [Mg<sup>2+</sup>] = 0.1 mM, [Aurora B] = 0.005 μg/μL in 20 mM tris pH 7.4 at room temperature. Separation buffer = 2 μM CX6 in 10 mM phosphate buffer, pH 7.4. Electric field strength = 662 V/cm

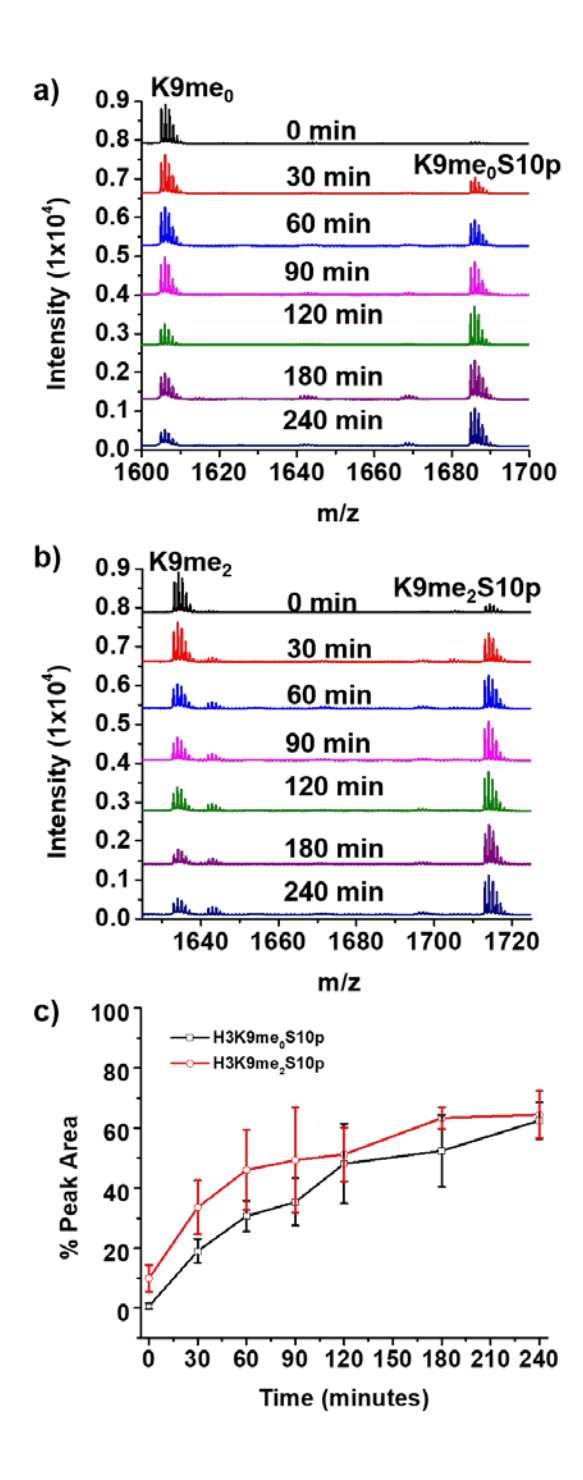


**Fig. S15 a** MALDI-TOF/TOF spectra with FAM-labeled H3K9me<sub>0</sub> substrate and FAM-labeled H3K9me<sub>0</sub>S10p product during an Aurora B kinase reaction over time. **b** MALDI-TOF/TOF spectra with FAM-labeled H3K9me<sub>2</sub> substrate and FAM-labeled H3K9me<sub>2</sub>S10p product during an Aurora B kinase reaction over time. **c** % peak area (FAM-labeled H3K9me<sub>x</sub>S10p; x=0,2; peptide peak over the total peak area) versus time using MALDI data. Reaction conditions: [peptide] = 10 μM, [ATP] = 20 μM, [Mg<sup>2+</sup>] = 0.1 mM, [Aurora B] = 0.005 μg/μL in 20 mM tris pH 7.4 at room temperature

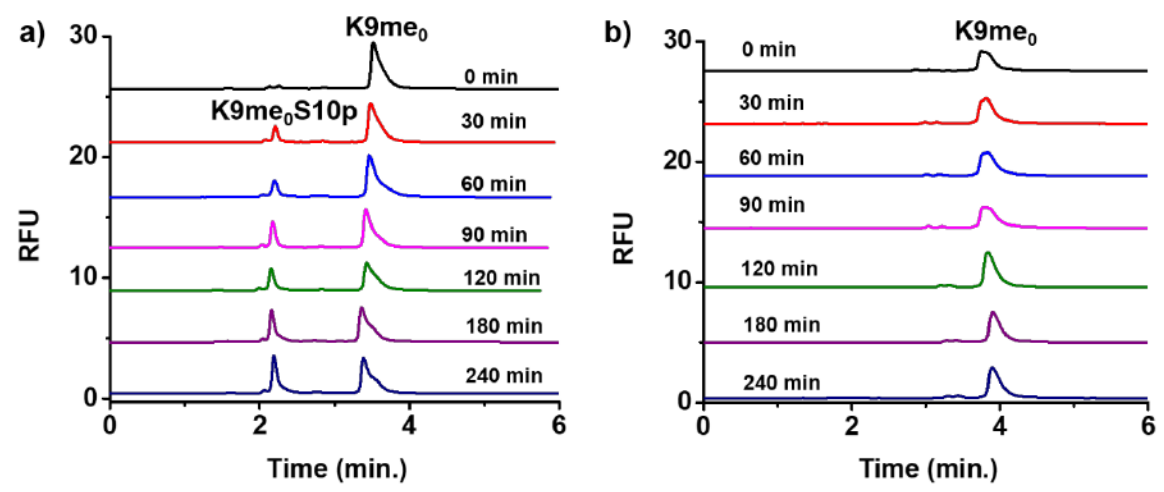


**Fig. S16 a** Separation of FAM-labeled H3K9me<sub>0</sub> substrate and FAM-labeled H3K9me<sub>0</sub>S10p product during an Aurora B kinase reaction in the absence of AZD1152-HQPA inhibitor. **b** Inhibition of FAM-labeled H3K9me<sub>0</sub>S10p product during an Aurora B kinase reaction in the presence of 2.5 nM AZD1152-HQPA inhibitor. Reaction conditions: [peptide] = 10 μM, [ATP] =  $20 \,\mu\text{M}$ , [Mg<sup>2+</sup>] =  $0.1 \,\text{mM}$ , [Aurora B kinase] =  $0.1 \,\mu\text{g}/\mu\text{L}$  in 20 mM tris pH 7.4 at room temperature. Separation buffer =  $2 \,\mu\text{M}$  CX6 in 10 mM phosphate buffer, pH 7.4. Electric field strength =  $662 \,\text{V/cm}$ 

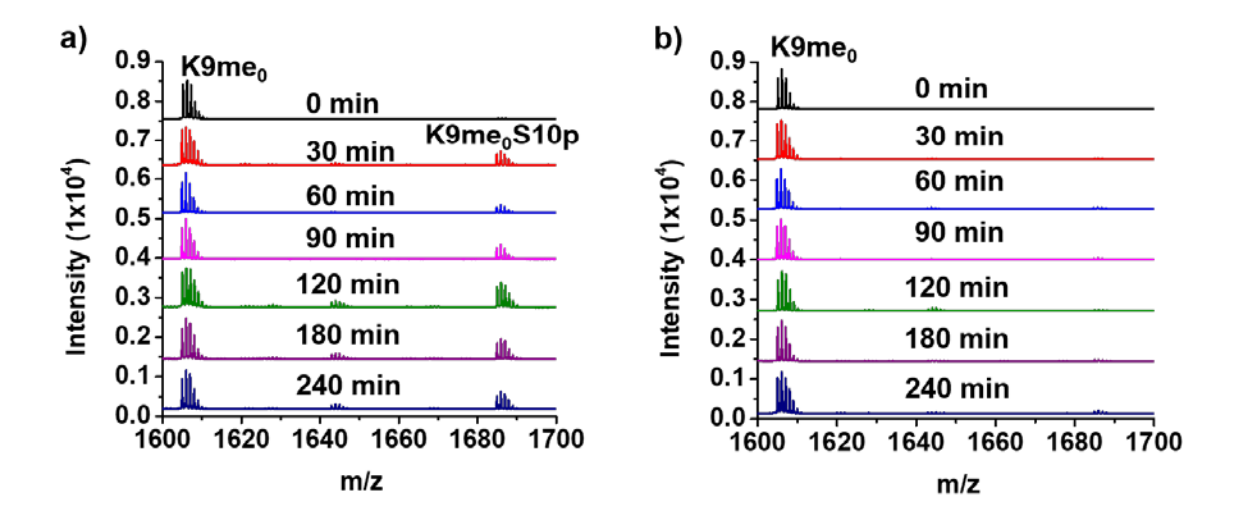


**Fig. S17 a** MALDI-TOF/TOF spectra with FAM-labeled H3K9me<sub>0</sub> substrate and FAM-labeled H3K9me<sub>0</sub>S10p product during an Aurora B kinase reaction over time with the absence of AZD1152-HQPA inhibitor. **b** MALDI-TOF/TOF spectra representing the inhibition of FAM-labeled H3K9me<sub>0</sub>S10p product during an Aurora B kinase reaction in the presence of 2.5 nM AZD1152-HQPA. Reaction conditions: [peptide] = 10  $\mu$ M, [ATP] = 20  $\mu$ M, [Mg<sup>2+</sup>] = 0.1 mM, [Aurora B kinase] = 0.1  $\mu$ g/ $\mu$ L, [AZD1152-HQPA] = 0 or 2.5 nM in 20 mM tris pH 7.4 at room temperature